Schweizerische Eidgenossenschaft
Confédération suisse
Confederazione Svizzera
Confederaziun svizra

Federal Department of the Environment,
Transport, Energy and Communications DETEC

Swiss Federal Office of Energy SFOE
Energy Research

Final report 31.01.2016

Potential of Thermoelectrics for Waste Heat Recovery

Date: 31.01.2016

Place: Bern

Contracting body:

Swiss Federal Office of Energy SFOE
Research Programme Electricity Technologies
CH-3003 Bern
www.bfe.admin.ch

Contractor:

Empa – Materials Science and Technology
Laboratory Materials for Energy Conversion
Überlandstrasse 129
CH-8600 Dübendorf
www.empa.ch

Fachhochschule Nordwestschweiz (FHNW)
Hochschule für Wirtschaft
Riggenbachstrasse 16
CH-4600 Olten
www.fhnw.ch

W. Neumann Consult AG (WNC)
Technopark Aargau
Dorfstrasse 69
CH-5210 Windisch
www.w-neumann.ch

Authors:

Dr. Corsin Battaglia, Empa, corsin.battaglia@empa.ch
Remo Widmer, Empa, remo.widmer@empa.ch
Prof. Thomas Helbling, FHNW, thomas.helbling@fhnw.ch
Léa Hug, FHNW, lea.hug@fhnw.ch
Dr. Barbara Miller, FHNW, barbara.miller@fhnw.ch
Wolfgang Neumann, W. Neumann Consult AG, info@w-neumann.ch
Max Götze, W. Neumann Consult AG, max.goetze@w-neumann.ch
Carole Sägesser, W. Neumann Consult AG, carole.saegesser@w-neumann.ch
Yannick Dubois, W. Neumann Consult AG, yannick.dubois@w-neumann.ch

SFOE Head of domain: Dr. Michael Moser, michael.moser@bfe.admin.ch
SFOE Programme manager: Roland Brüniger, roland.brueniger@r-brueniger-ag.ch
SFOE Contract number: SI/501211-01

Swiss Federal Office of Energy SFOE
Mühlestrasse 4, CH-3063 Ittigen; Postal address: CH-3003 Bern
Phone +41 58 462 56 11 · Fax +41 58 463 25 00 · contact@bfe.admin.ch · www.bfe.admin.ch

Abstract

Thermoelectrics enables the direct conversion of heat flux into electrical energy. The aim of this study is to provide an up-to-date assessment of the technical and economic feasibility of using thermoelectric converters for waste heat recovery. As a basis for this study an overview on the state of development of the different thermoelectric material classes is given. Market opportunities for currently available and future thermoelectric materials are identified and compared to competing processes.

It is shown that for stationary applications, thermoelectric generators can rival competing technologies such as heat transfer or cycle processes to generate electric energy only in the temperature range below 65°C. Of special interest is the field of cooling in building technology since here, payback times of up to 20 years are accepted and thermoelectric generators convince by long life times. Within the current project, a pilot plant was developed for testing thermoelectric generators for applications in building technologies.

Zusammenfassung

Die Thermoelektrik erlaubt die direkte Umwandlung von Wärmeströmen in elektrische Leistung. Ziel dieser Studie ist eine aktuelle Einschätzung der technischen und wirtschaftlichen Machbarkeit der Abwärmenutzung durch thermoelektrische Konverter. Als Grundlage für die Studie wurde ein aktueller Überblick über den Status der einzelnen thermoelektrischen Materialsysteme erarbeitet. Marktchancen für aktuell verfügbare und zukünftige thermoelektrische Materialien werden identifiziert und mit Konkurrenzprozessen verglichen.

Es zeigt sich, dass thermoelektrische Generatoren für stationäre Anwendungen nur im Temperaturbereich unter 65°C konkurrierenden Prozessen wie Wärmeverschiebung oder die Erzeugung von Strom durch Kreislaufprozesse überlegen sein können. Besonderes Interesse gilt dem Bereich der Kühlung in der Gebäudetechnik, da hier generell Payback Zeiten von bis zu 20 Jahren akzeptiert werden und thermoelektrische Generatoren durch Langlebigkeit bestechen. Zur Weiterführung dieser Arbeit wurde ein Demonstrationsmodell entwickelt, an dem thermoelektrische Generatoren für den Gebäudebereich im Pilotmassstab getestet werden können.

Résumé

La thermoélectrique permet de générer un courant électrique directement à la base d'un flux de chaleur. Le but de cette étude est une évaluation critique de la faisabilité technique et économique au sujet de la récupération de chaleur résiduelle par des convertisseurs thermoélectriques. Comme base pour cette étude, le statut de développement actuel des différentes classes de matériaux thermoélectriques est résumé. Le marché des matériaux thermoélectriques disponibles actuellement et en future est identifié et comparé avec des procès concurrents.

Il s'avère que pour des installations stationnaires, les générateurs thermoélectriques sont supérieurs aux procès compétitifs comme le déplacement de chaleur ou la production de courant électrique par des procès de circulation uniquement à des températures inférieures à 65°C. Particulièrement à considérer est le champ d'application de réfrigération dans la technique de bâtiment. Ceci est d'un côté parce que un temps de remboursement jusqu'à 20 ans est accepté et d'un autre côté grâce à la longue durée de vie des générateurs thermoélectriques. Dans le cadre de ce projet, un modèle de démonstration a été construit qui permet de faire des tests pour évaluer l'application dans la technique de bâtiment.

Table of content

1. Introduction

Heat generated by industrial processes, urban facilities, data centers, etc. is ubiquitous. Much effort has been devoted to develop heat management strategies that maximize energy efficiency. Conceptually there are two different approaches to create value from heat. Heat can either be transferred and utilized again in the form of heat in another location or heat can be converted into electrical energy, via e.g., water steam or organic Rankine cycles or thermoelectrics. Thermodynamics dictates a maximum conversion efficiency equal to the Carnot efficiency for heat conversion processes. While certain organic Rankine cycle technologies operate very close to the Carnot limit, heat transfer approaches remain very attractive, as, besides heat losses, which can be minimized by appropriate thermal insulation strategies, the full energy contained in heat can be utilized.

The aim of this study is to assess the potential of thermoelectrics for waste heat recovery. Waste heat is defined as the part of heat that cannot be recovered with today's technologies and does not serve an intentional heating purpose.[1] The main advantages of thermoelectric heat to electricity conversion compared to other technologies include high reliability, low maintenance, small size and no noise and vibrations. These characteristics have qualified thermoelectrics as energy source for many deep space missions. The main disadvantage of thermoelectrics is the relatively low conversion efficiency. For a fictive thermoelectric material with temperature independent physical properties and thermoelectric figure of merit equal to unity, the highest achievable efficiency is about 20% of the Carnot efficiency. Consequently under many circumstances, thermoelectrics is not competitive with water steam and organic Rankine cycles.[2]

Nevertheless this study identifies potential applications where thermoelectrics offer a distinct advantage over competing technologies. Besides the technical feasibility, we also investigate the economic potential by determining production and target cost.

2. Status of thermoelectric materials research

2.1 What makes a 'good' thermoelectric material?

The thermoelectric figure of merit zT is defined by

$$zT = \frac{\sigma S^2 T}{\kappa_e + \kappa_l}$$

where σ is the electrical conductivity (in S/cm), S the Seebeck coefficient (in μV/K), T the absolute temperature (in K), and κ_e and κ_l the electronic and lattice contributions to the thermal conductivity (in W/m·K). Both σ and S, and consequently κ_e, which is proportional to σ through the Wiedemann-Franz law, depend on the charge carrier density n (in cm^{-3}) or more fundamentally on the chemical potential. Carrier concentration can be optimized for maximum zT through doping, i.e. substitution of elements of the host crystal with elements that carry either one more or one less electrons, called donors or acceptors respectively. At optimum zT, carrier concentration typically lies in the range of 10^{19} to 10^{20} cm^{-3} for most thermoelectrics.

Within the relaxation time approximation to the Boltzmann transport equations, zT can be rewritten in terms of functions u and v that depend on the chemical potential and a function β that does not depend on the carrier concentration.

$$zT = \frac{u\beta}{v\beta + 1}$$

β is often called the thermoelectric quality factor and takes the form[3]

$$\beta = \left(\frac{k_B}{e}\right)^2 \cdot \frac{2e(k_B T)^{3/2} T}{(2\pi)^{3/2} hbar^3} \frac{\mu_0 m_{DOS}^{*3/2}}{\kappa_l}$$

where μ_0 is the mobility of charge carriers in a defect free, non-degenerate material and m^*_{DOS} is the density of states effective mass. Assuming that optimum carrier concentration can be reached, maximizing β maximizes zT. As pointed out by Wang et al.[4] this expression assumes that the scattering mechanism remains unchanged when doping is increased. As practical

thermoelectrics are degenerate semiconductors, μ_0 should be determined on appropriately doped rather than on undoped samples. Another important point is that μ_0 also depends on the effective mass m^*_{DOS}. For thermoelectrics above room temperature, scattering by acoustic phonons usually dominates, in this case μ_0 is inversely proportional to $m^{*5/2}_{DOS}$. Consequently β scales as m^{*-1}_{DOS} meaning that materials with lower effective carrier mass should be better thermoelectrics. For materials with a Fermi surface consisting of several degenerate valleys, m^*_{DOS} needs to be replaced by $N_V^{2/3} \cdot m^*_{DOS}$ where N_V is the valley degeneracy. Good thermoelectric materials should have a small single valley density of states effective mass to maintain high mobility and consequently high conductivity, but a large total density of states effective mass caused by a large degeneracy N_V resulting in increased entropy for the charge carriers and consequently larger Seebeck coefficient, which can be understood as being the entropy per charge carrier.[5]

Furthermore a good thermoelectric material should minimize the lattice contribution to the thermal conductivity. Phonons carry heat over a broad spectrum of frequencies ω and the lattice contribution to the thermal conductivity can be expressed as an integral of contributions over the frequency spectrum. Each contribution is of the form $\kappa_l(\omega)=C_p(\omega)\cdot v^2(\omega)\cdot\tau(\omega)$, where $C_p(\omega)$ is the specific heat of phonons, $v(\omega)$ their velocity, and $\tau(\omega)$ their relaxation time. In the Debye approximation, $C_p(\omega)$ scales with ω^2. The first strategy to reduce the thermal conductivity due to phonons is to use heavy elements resulting in high average atomic mass as the velocity of acoustic phonons is inversely proportional to the square root of the mass of the atoms. The second strategy is to scatter phonons. The scattering rate τ^{-1} for Umklapp scattering depends quadratically on phonon frequency ω^2, resulting in conjunction with the Debye approximation in a frequency independent contribution to the thermal conductivity. Point defects with high mass contrast result in a scattering rate τ^{-1} that scales with ω^4, thus scatters strongly the high frequency phonons. Scattering at grain boundaries targets the

low frequency phonons with a constant, frequency independent scattering rate τ^{-1}~cst. Scattering of mid-frequency phonons with $\tau^{-1} \sim \omega^3$ can be achieved e.g. by introducing an array of nm-sized dislocations.

2.2 Energy conversion efficiency calculated from the thermoelectric figure of merit

The expression commonly used to determine the maximum efficiency of a thermoelectric generator was first derived by Altenkirch[6] assuming temperature independent material properties. In Ioffe's formulation[7] the expression for the maximum efficiency takes the form

$$\eta_{max} = \frac{\Delta T}{T_h} \frac{\sqrt{1 + zT_{avg}} - 1}{\sqrt{1 + zT_{avg}} + \frac{T_c}{T_h}}$$

where T_h and T_c are the temperatures on the hot side and cold side respectively, ΔT the difference between T_h and T_c, and zT_{avg} the average zT over the temperature interval. When ρ, S, and κ depend on temperature, the expression only provides reliable results for small ΔT. Nevertheless, the expression has often been applied to large temperature differences in the literature, which may result in incorrectly large efficiencies.

To avoid solving the complex differential heat current equation numerically, Kim et al. recently introduced a methodology to calculate the efficiency of a thermoelectric generator when operated over a large temperature difference taking into account conduction heat, Joule heat, Peltier heat as well as Thomson heat.[8] The approach yields the expression above for temperature independent materials properties as required. In what follows we review some of the most important thermoelectric materials. Resistivity, Seebeck coefficient, and thermal conductivity of important best-in-class thermoelectric materials were extracted from literature and used to calculate the maximum efficiency following the approach of Kim et al.

It is important to note that these efficiencies represent the efficiency of a single thermoelectric leg. Importantly, when designing a thermoelectric module, a compatible pair of p-

type and n-type material must be chosen. The efficiency is maximized when the reduced current density defined as the ratio of electrical current to the heat flux is equal to the compatibility factor.[9] Materials with similar compatibility factors are essential when combined into segmented legs. For serially connected p- and n-type legs, both legs can be made to operate at maximum efficiency by adjusting the relative cross sectional area of the legs. Losses due to electrical and thermal contact resistances are not taken into account.

2.3 Status of material classes

Bismuth tellurides

Alloys based on bismuth tellurides (Bi_2Te_3) and antimony tellurides (Sb_2Te_3) have been employed for thermoelectric applications since the 1950s.[10] For bismuth- and tellurium-rich compositions, the most favorable native defects are bismuth- and tellurium antisite defects acting as acceptors and donors respectively. Consequently bismuth-rich samples typically exhibit p-type conduction, while tellurium-rich samples typically result in n-type behavior. The valley degeneracy for both the valence and the conduction band is 6.

The heavy mass of the constituent atoms leads to phonons with relatively low frequency resulting in a relatively low thermal conductivity. The introduction of atomic disorder with high mass contrast, e.g. by replacing bismuth with isovalent antimony or tellurium with isovalent selenium, led early to peak zT values near unity. Point defects are efficient in scattering high frequency phonons, although the high frequency part of the phonon spectrum only contributes relatively little to the thermal conductivity.

In 2008, combining ball milling and hot pressing, Poudel et al. demonstrated p-type nanostructured bulk $Bi_{0.5}Sb_{1.5}Te_3$ with peak zT values of 1.4 at 100°C (see Fig. 1).[11] The zT enhancement is primarily due to a substantial reduction in thermal conductivity resulting from phonon scattering at the nanosized, randomly oriented, closely packed, highly crystalline grains with very clean grain boundaries. Grain boundaries are very efficient in scattering the

low frequency phonons, which contribute strongly to the thermal conductivity. The approach by Poudel et al. is potentially low cost and scalable to large volumes.

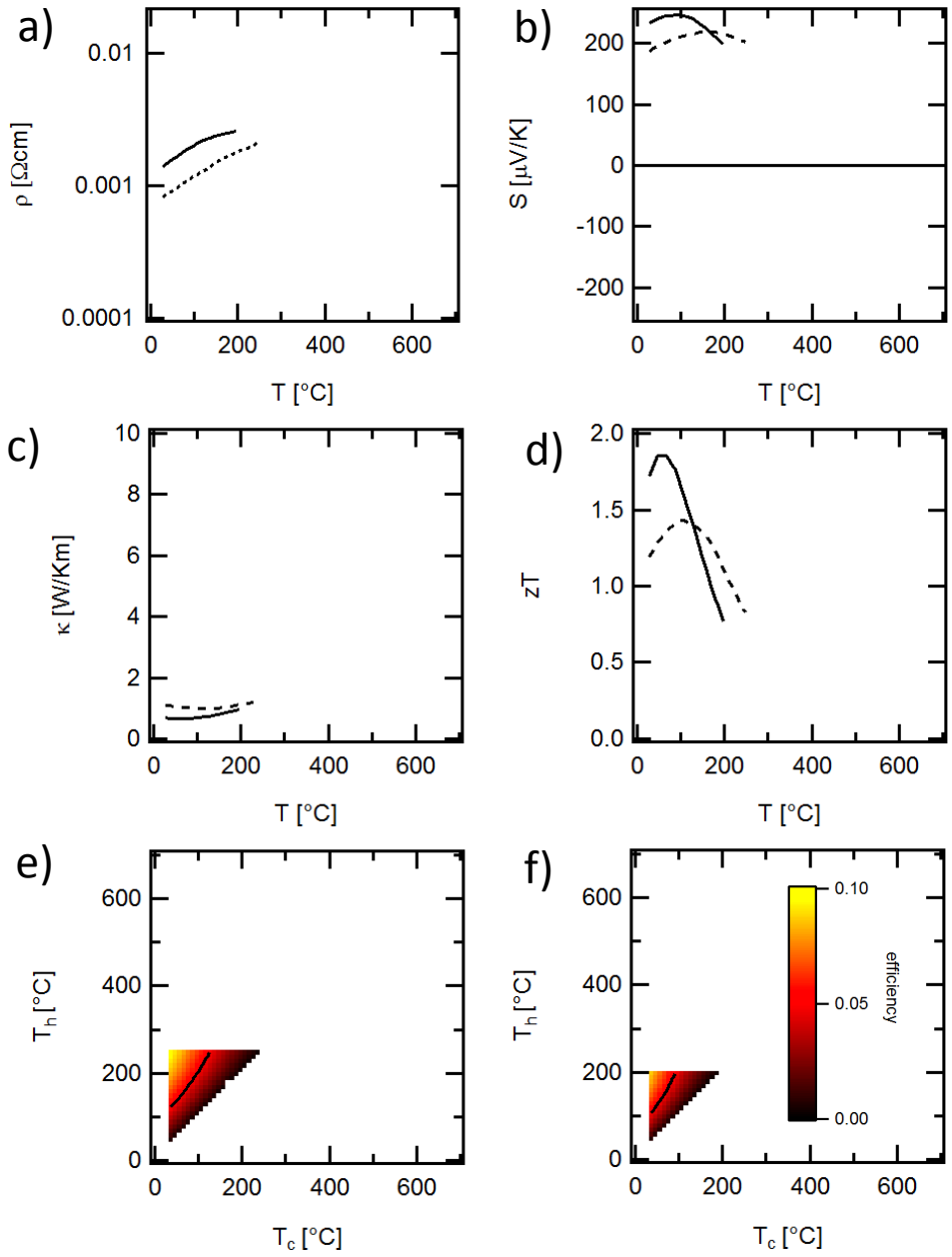

Fig. 1 Comparison between ball milled[11] (dashed line) and melt spun[12] (continuous lines) Bi_2Te_3: (a) resistivity, (b) Seebeck coefficient, (c) thermal conductivity, (d) zT, (e) calculated efficiency for ball milled Bi_2Te_3, (f) calculated efficiency for melt spun Bi_2Te_3. Contour lines for 5% efficiency are also shown in (e) and (f).

Scattering phonons over the full spectral range is key to further reduce the thermal conductivity κ. However, only phonon scattering strategies that maintain a high charge carrier mobility μ lead to high zT values, as zT is determined by the ratio of μ/κ. Kim et al recently applied a liquid phase sintering technique under applied pressure and transient flow to $Bi_{0.5}Sb_{1.5}Te_3$ creating a periodic dislocation array with a typical spacing of only a few nanometers that scatter the mid-frequency phonons resulting in substantial reduction of the thermal conductivity and a reproducible peak zT of 1.86 near 50°C.[12] According to the authors, their approach is highly scalable and also applicable to other thermoelectric material systems including lead telluride, skutterudites and silicon/germanium alloys.

Even higher zT values were determined by Venkatasubramanian et al. through transport measurements along the cross-plane direction for epitaxially grown Bi_2Te_3/Sb_2Te_3 superlattices grown by low-temperature organometallic epitaxy on GaAs wafers.[13,14] However, this method is expensive and not compatible with large volume manufacturing.

Skutterudites

The physics of skutterudite thermoelectrics of general formula $R_xCo_4Sb_{12}$ is governed by rattler atoms R filling the icosahedral interstitial sites of the skutterudite structure. The addition of the rattler atoms reduces the thermal conductivity due to alloying disorder and the modification of the phonon spectrum while simultaneously doping the host material. zT values in excess of 1 have been reported for single-element filling (Na[15], Ba[16], In[17], Ce[18], etc.) and multiple filling (Sr, In, Ba, La, Ce, Yb, etc.[19,20,21,22]).

Rogl et al. demonstrated zT values of up to 1.6 at 560°C for n-type $Sr_{0.09}Ba_{0.11}Yb_{0.05}Co_4Sb_{12}$ with a total filling fraction of 25% using a combination of melting in evacuated quartz tubes and arc melting in combination with ball milling and hot pressing (see Fig. 2).[21] Using a similar process followed by prolonged annealing at 570°C, p-type skutterudites with composition $DD_{0.59}Fe_{2.7}Co_{1.3}Sb_{11.8}Sn_{0.2}$, where DD stands for didymium, a

mixture of the elements praseodymium and neodymium, reached a zT of 1.3 at 500°.[22] Even higher zT values were obtained by applying a high-pressure torsion, but this phenomenon is not yet well understood and difficult to scale.[21,22]

Tang et al. recently demonstrated that the effective valley degeneracy of the conduction band of n-type skutterudites increases from 3 to 15 as an additional electron pocket with 12 fold degeneracy 110 mV above the conduction band edge becomes occupied at higher temperature explaining the good performance of skutterudites.[23]

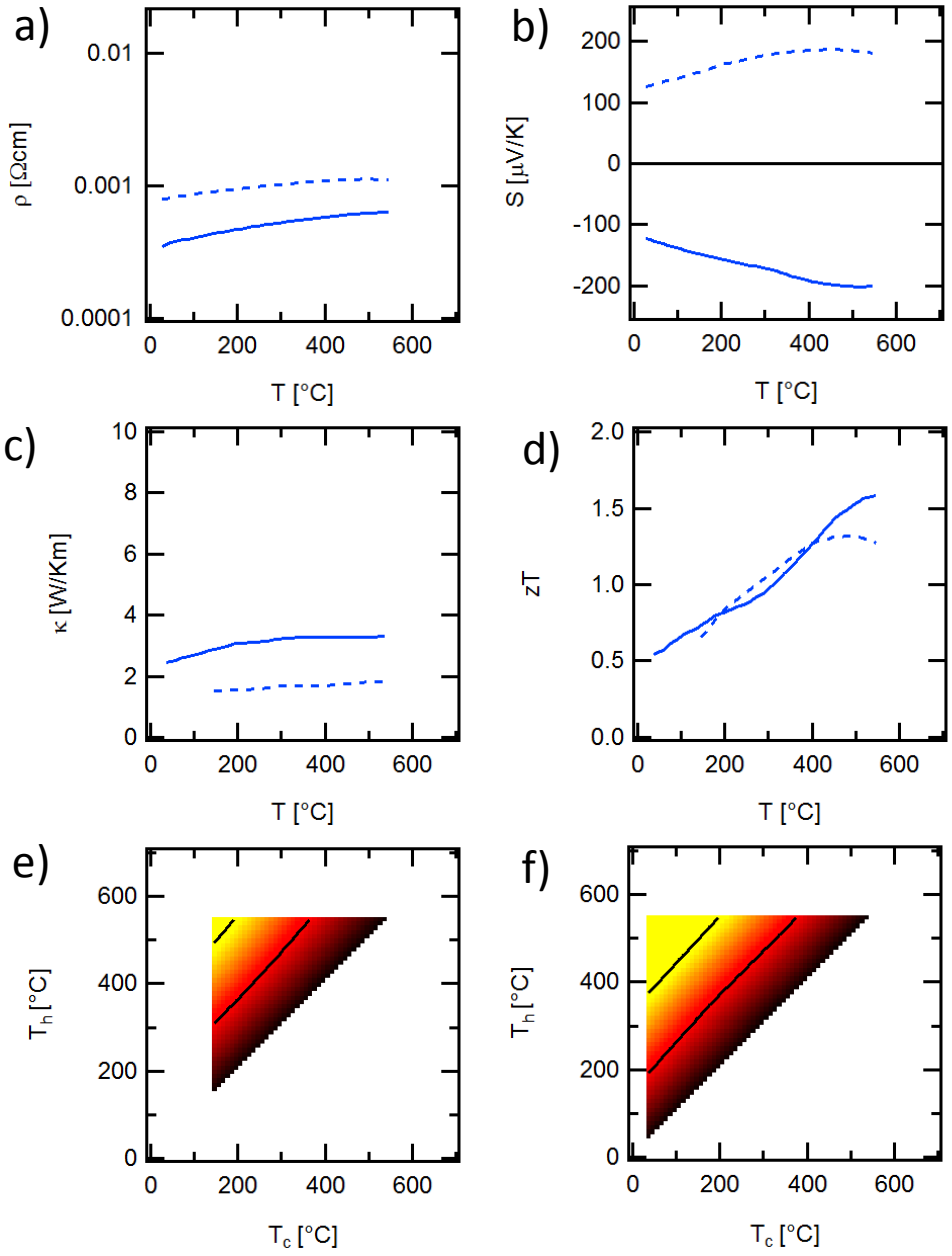

Fig. 2 Comparison between p-type[22] (dashed line) and n-type[21] (continuous line)

skutterudites. (a) resistivity, (b) Seebeck coefficient, (c) thermal conductivity, (d) zT, (e) calculated efficiency of p-type skutterudite, (f) calculated efficiency of n-type skutterudite. The color scale is identical to the one in Fig. 1. Contour lines for 5% and 10% efficiency are also shown in (e) and (f).

Half-Heuslers

Intermetallic Half-Heusler alloys consist of three metals X, Y, Z with 1:1:1 composition, where the Y and Z atoms are arranged in a zinc blende sublattice with the X atoms filling every second tetrahedral interstitial site. Half-Heuslers with 18 valence electrons exhibit semiconducting behavior.[24] The stability and formation of a band gap can be understood within a simplified purely ionic picture in which the most electropositive element X transfers its valence electrons to the more electronegative elements Y and Z, forming the covalently bonded zinc blende sublattice. A typical example is TiNiSn, where Ti provides its 4 valence electrons (from $3d^2 4s^2$ to $3d^0$) to close the d-shell of Ni (from $3d^8 4s^2$ to $3d^{10}$) and p-shell of Sn (from $5s^2 5p^2$ to $5s^2 5p^6$).

Half-Heusler thermoelectrics typically feature relatively high Seebeck coefficients (200-350 μV/K, see Fig. 3). The valley degeneracy for the conduction band of TiNiSn half-Heuslers is 3. In principle aliovalent dopant atoms can be introduced on any of the three sites to adjust the carrier density (e.g. Sb acts as a donor on the Sn site in TiNiSn) resulting in resistivities on the order of a few 10^{-3} Ω/cm. The main challenge for Half-Heusler thermoelectrics is their relatively high thermal conductivity of up to 10 W/m·K. The thermal conductivity can be reduced by introducing isovalent atoms with large mass contrast (e.g. Zr or Hf on the Ti site in TiNiSn) resulting in scattering of the high frequency phonons.

Combining this approach with ball milling and hot pressing, Sakurada and Shutoh were able to reduce the thermal conductivity of n-type (Ti,Zr,Hf)NiSn alloys to about 3 W/m·K resulting in high zT values peaking at 1.45 at 430 °C.[25] This result has not been re-

produced so far. Culp et al. obtained a zT of 0.8 at 800°C (0.5 at 430°C) using arc melting. Employing levitation melting, Yu et al. were able to reach a zT value of 1 at about 700°C (0.7 at 430°C).[26]

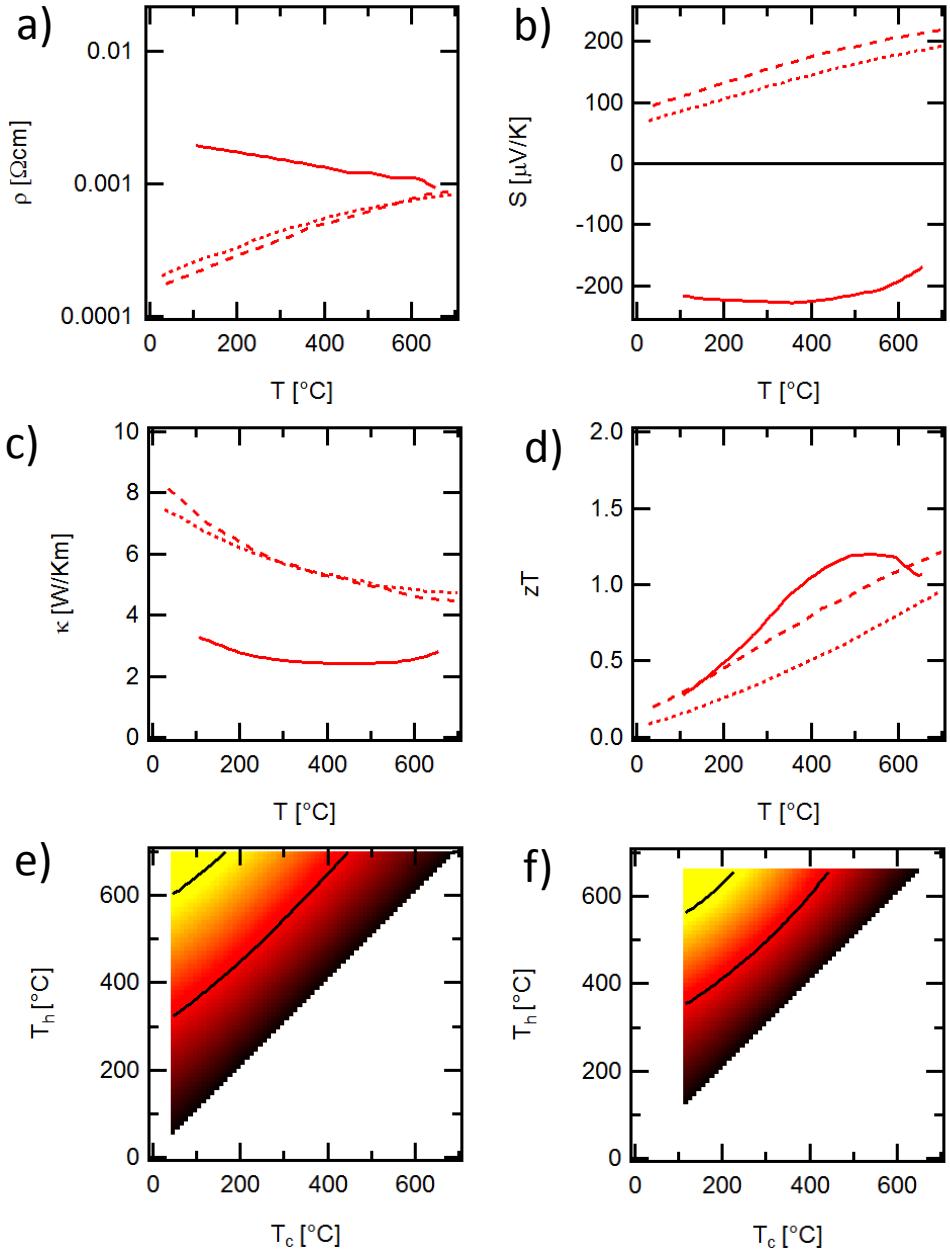

Fig. 3 Comparison between p-type (dashed line[34], dotted line[33]) and n-type (continuous line[30]) half-Heuslers. (a) resistivity, (b) Seebeck coefficient, (c) thermal conductivity, (d) zT, (e) calculated efficiency of p-type half-Heusler, (f) calculated efficiency of n-type half-Heusler. The color scale is identical to the one in Fig. 1. Contour lines for 5% and 10% efficiency are also shown in (e) and (f).

Similarly Joshi et al. employed arc melting to reach a zT value near 1 at 600-700°C.[27] Makongo et al. elucidated the formation of (Zr,Hf)Ni_2Sn full-Heusler inclusions with typical sizes below 10 nm in the (Zr,Hf)NiSn half-Heusler that scatter the mid-frequency phonons. In particular the formation of coherent phase boundaries between half- and full-Heusler guarantees that carrier mobility remains high.[28] Populoh et al. observed that (Ti,Zr,Hf)NiSn is not phase stable but separates into Ti-rich/(Zr,Hf)-deficient and Ti-deficient/(Zr,Hf)-rich phases respectively at a characteristic length scale of about 20 μm helping to scatter the low-frequency phonons resulting in a zT value close to 1 at 450°C.[29] Using the same material system, Schwall and Balke were able to produce material with zT values of up to 1.2 at 550°C (1.1 at 450°C), which gives some hope that the results of Sakurada and Shutoh may be reproduced one day.[30]

The performance of p-type Half-Heusler has somewhat been lacking behind their n-type counterparts. Within the TiCoSb system employing isovalent Zr and Hf substitution on the Ti site for phonon scattering and aliovalent Sn substitution on the Sb site for p-type doping , Culp et al. demonstrated a p-type half-Heusler with zT of about 0.5 at 700°C (0.25 at 430°C). In 2014, Fu et al. reported a zT of 0.8 at 630°C (0.7 at 430°C) for p-type $FeV_{0.6}Nb_{0.4}Sb$ half-Heuslers with Ti acceptors on the V/Nb site.[31] Importantly, this result was confirmed shortly after by Joshi et al. who demonstrated a zT near 1 at 700° (0.65 at 430°C) for the same material system.[32] However, the limited solubility of Ti dopants on the V/Nb site limits the performance of this material system as the optimal carrier concentration cannot be reached.[33] Eliminating V improves the carrier mobility at high temperatures and allows optimum Hf doping enabling a zT close to 1.5 at 930°C (0.85 at 430°C) for $FeNb_{0.86}Hf_{0.14}Sb$, where Hf acts as an acceptor on the Nb site.[34]

Silicides

Among the large class of silicides, Mg_2Si represents a promising system for thermoe-

lectric applications. Mg_2Si crystallizes in the antifluorite structure, in which Si atoms occupy a face-centered cubic lattice with Mg atoms occupying the eight tetrahedral sites in the interior of the unit cell. In particular the n-type $Mg_2(Si,Sn)$ system showed high zT values of up to 1.1 at 480°C for Sb-doped $Mg_2Si_{0.4}Sn_{0.6}$[35], 1.3 at 430°C for Sb-doped $Mg_2Si_{0.3}Sn_{0.7}$[36], and 1.4 at 530°C for Bi-doped $Mg_2Si_{0.53}Sn_{0.4}Ge_{0.05}Bi_{0.02}$.[37] The latter sample was synthesized melted from elemental powders in evacuated quartz tubes, followed by ball milling and hot pressing.

Mg_2Si and Mg_2Sn both exhibit an indirect band gap with the valence band maximum at the Brillouin zone center and the three-fold degenerate conduction band minimum at the X point. For Mg_2Si, the lowest lying conduction band consists of light electrons, but with a second conduction band of heavier electrons about 200 meV above. For Mg_2Sn, the situation is reversed with a light electron band about 400 meV above the lower lying heavier electron band. Highest zT is achieved for compositions for which the two bands converge, doubling the valley degeneracy and leading to Seebeck coefficients up to -250 μV.[36] Sb and Bi, both act as electron donors. The resistivity is in the range of $0.5\text{-}1.5\cdot10^{-3}$ Ω·cm.

Sn and Ge isovalently substitute Si and contribute the phonon scattering through their mass difference. The thermal conductivity reduces from 11 W/m·K for Mg_2Si to below 2-3 W/m·K for $Mg_2Si_{0.53}Sn_{0.4}Ge_{0.05}Bi_{0.02}$.

Tetrahedrites

Excellent thermoelectric properties have been discovered only recently in $Cu_{12}Sb_4S_{13}$ tetrahedrite semiconductors, so far not yet considered for thermoelectric applications.[38] The complex crystal structure features two symmetry inequivalent Cu sites with tetrahedral and trigonal coordination by S and Sb atoms with trigonal coordination by S. In this configuration Sb carries a s^2 lone pair resulting in a strong anharmonicity, which has been identified to be responsible for the remarkably low lattice thermal conductivity. Undoped $Cu_{12}Sb_4S_{13}$ features a thermal conductivity in the range of 1.2-1.5 W/m·K. For doped samples, the conductivity

decreases to below 0.8 W/m·K as the electronic contribution to the thermal conductivity reduces.[39] In fact, undoped $Cu_{12}Sb_4S_{13}$ is a weekly metallic, degenerately doped p-type semiconductor, while $Cu_{10}Zn_2Sb_4S_{13}$ is an insulator. All Cu atoms were determined to be in a

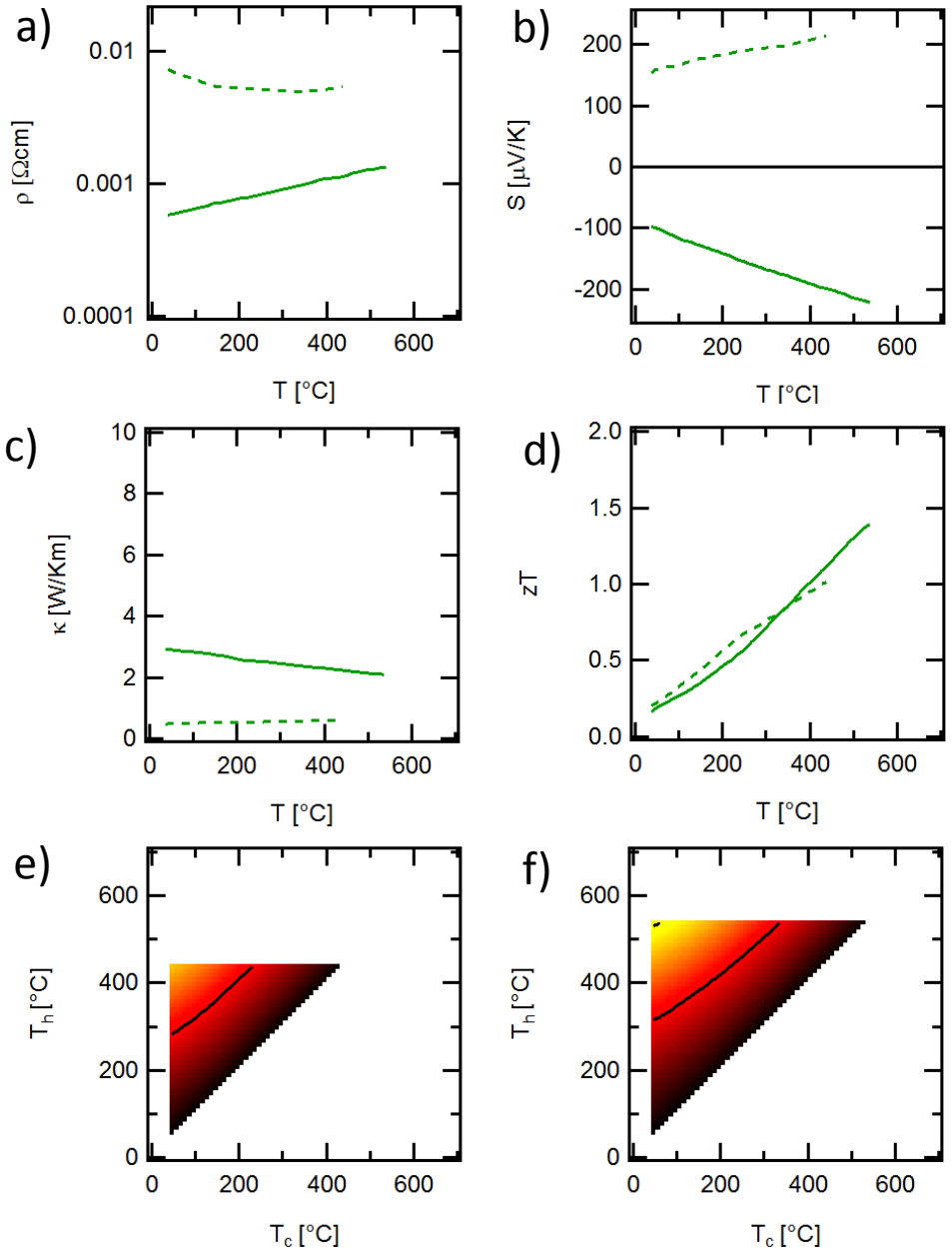

Fig. 4 Comparison between p-type tetrahedrite[38] (dashed line) and n-type magnesium silicide[35] (continuous line[30]). (a) resistivity, (b) Seebeck coefficient, (c) thermal conductivity, (d) zT, (e) calculated efficiency of p-type tetrahedrite (e) and for magnesium silicide (f). The color scale is identical to the one in Fig. 1. Contour lines for 5% and 10% efficiency are also shown in (e) and (f).

monovalent Cu^{1+} state, while Zn is in a Zn^{2+} state. Ni and Zn codoping leads to p-type $Cu_{10.5}Ni_{1.0}Zn_{0.5}Sb_4S_{13}$ with excellent zT values slightly above 1 at 430°C.[40] Ni prefers to substitute Cu on the tetrahedral site and is believed to be in a N^{1+} state. A high Seebeck coefficient in the range of 200 μV/K is obtained by moving the Fermi level close to the valence band where the density of states exhibits a strong peak and consequently a strong energy dependence which increases the configurational entropy as many states are available within a small energy interval. At optimal doping, resistivities are on the order of $5\text{-}8\cdot10^{-3}$ Ohm·cm.

Other materials

MgAgSb has been reported as early as in 1941[41], but its thermoelectric properties have only been investigated recently by Kirkham et al.[42] and more recently by Zhao et al.[43]. MgAgSb takes a Half-Heusler structure above 360°C, a Cu_2Sb-related structure at temperatures between 300°C and 360°C, and a tetragonal structure from room temperature up to 300°C. These structural phase transitions correlate with the discontinuous abrupt changes in the temperature dependence of the Seebeck coefficient and the electrical resistivity. Zhao et al. employed a two-step ball milling procedure combined with hot pressing to demonstrate zT values exceeding values of 1 already at 100° for $MgAg_{0.97}Sb_{0.99}$ and reaching values of almost 1.4 for MgAg0.965Ni0.005Sb0.99 for a relatively broad plateau between 175°C and 275°C. What is remarkable about this result is the high zT values at so low temperatures. The zT maxima fall midway in temperature between the zT maxima of Bi_2Te_3 and PbTe. The thermal conductivity remains below 1 W/m·K up to 250°C. Li et al. suggested that the surprisingly low thermal conductivity can be explained by the relatively low activation energies for Ag^+ and Mg^{2+} ion migration in the structure against a stiff Sb framework, leading to dynamic atomic disorder, which is very efficient in scattering phonons. A similar mechanism although with only one mobile ion species has been suggested for $Cu_{2-x}Se$, which reaches a zT of 1.5 at 725°C.[44] The Seebeck coefficient is remarkably high, between 200-250 μV/K, thus MgAgSb

exhibits p-type behavior. A n-type partner with compatible properties has not been discovered so far. While MgAgSb cannot be considered a viable economic alternative to say Bi_2Te_3 due to the high cost of silver of 600$/kg[45], which is more than 5x more expensive than the cost of the already very expensive tellurium, this material nevertheless proved that new materials with very interesting thermoelectric properties can be (re)discovered.

PbTe and other lead chalcogenides provide high performance, but are prohibited in Europe by the directive on the restriction of the use of certain hazardous substances in electrical and electronic equipment in particular for thermoelectric applications.[55] The interested reader is referred to a recent review by Zhao et al.[46]

Oxides still exhibit comparatively low zT values and are only relevant for very high temperature applications, where nevertheless processes competing with thermoelectrics are typically more efficient. The interested reader is directed to a recent review by Populoh et al.[47] as well as to recent reports of the CCEM and BFE co-funded project HITTEC.

The family of organic-inorganic halide perovskites has recently attracted tremendous interest from the photovoltaic community with demonstrated solar cell power conversion efficiencies above 20%. More recently these materials are also considered for thermoelectric applications with zT values of up to 0.13 at room temperature.[48] Stabilizing organic-inorganic halide perovskites for realistic thermoelectric application environments is expected to be a considerable challenge.

Readers interested in the use of polymers and polymer composites for thermoelectric applications are directed to a recent review by Culebras et al.[49]

Recent work by Keppner et al. evaluating the use of ionic liquids as active components for thermoelectrics can be found in Ref. 50.

2.4 Economic and political factors affecting raw materials price and supply

Several thermoelectric materials described above are made from elements that are

either critical, rare or toxic. In this section, we summarize some key points concerning the availability, cost and/or toxicity of these elements.

Tellurium

With an abundance in the earth's crust of only 0.001 ppm, tellurium is three to four times less abundant then gold and platinum respectively. Consequently tellurium is expensive and currently costs about 117 $/kg.[51] Tellurium is a byproduct of copper mining. Besides for thermoelectric applications, tellurium is mainly used in cadmium telluride thin film solar cells with typical absorber thicknesses on the order of 1 μm that own about 10% of the world photovoltaic market. The official report on critical raw materials for the European Union assesses the supply risk and economic importance for tellurium similarly to copper and consequently not critical to the European Union (see Fig. 5).[52]

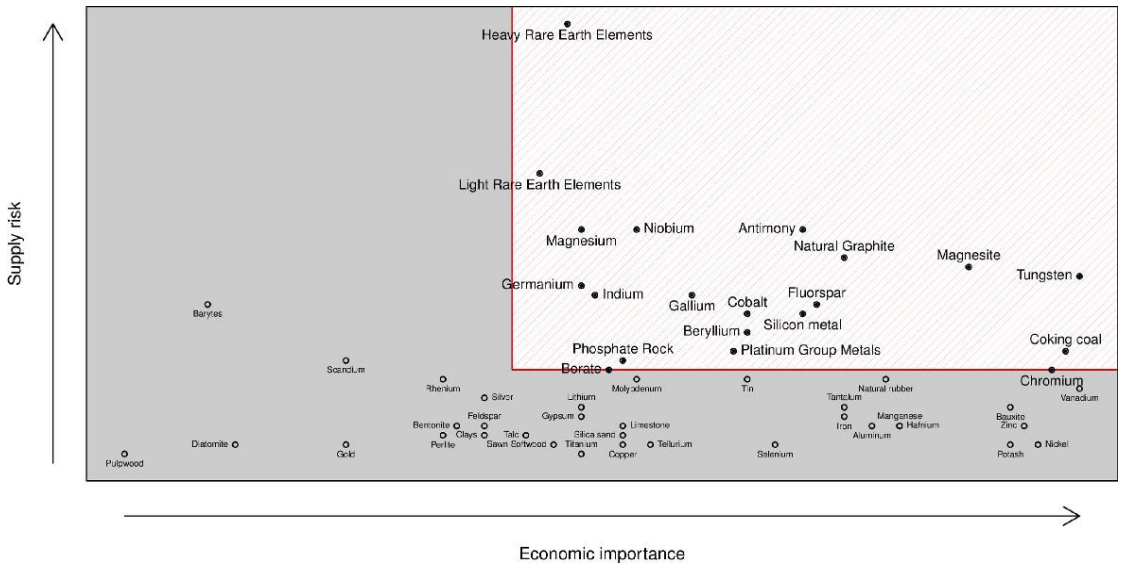

Fig. 5: Criticality assessment carried out by the European Commission at EU level covering 54 materials. Economic importance is derived from the proportion of each material associated with industrial megasectors, combined with its gross value added to EU GDP. Supply risk uses the World Governance Indicator taking into account political stability and absence of violence, government effectiveness, regulatory quality, and rule of law.[52]

Bismuth

Bismuth is a byproduct of lead mining. Its abundance in the earth crust is 0.025 ppm. Compared to its lower mass heavy metal neighbors in the periodic table mercury, lead, and thallium, it is surprisingly non-toxic and finds application as a replacement for lead in brass and solder and in pharmaceutical products. Current price is about 25 $/kg.[53]

Lead

Lead is abundant with 10 ppm in the earth's crust and cheap at about 2$/kg.[54] Today, lead is mostly used in lead acid batteries. While lead was also used for many other applications, it has been banned due to its high toxicity. The directive on the restriction of the use of certain hazardous substances in electrical and electronic equipment was adopted in 2003 by the European Union and took effect in 2006.[55] It precludes the use of lead in most electrical and electronic applications Exceptions include lead in specific solders and cadmium telluride photovoltaic modules. No exception is specified for thermoelectric generators.

Cobalt

Cobalt is an abundant element with 30 ppm in the earth's crust. The primary use of cobalt is for rechargeable lithium ion battery cathodes, but cobalt finds also numerous other industrial applications. China is the world's leading producer of cobalt, but 50% of the global production of cobalt in 2014 originally comes from Congo, where also the largest world reserves (almost 50%) are found. The European Commission classifies cobalt as critical. Current price is about 30$/kg.[56]

Antimony

The main use of antimony is as hardener of lead in lead acid batteries and as a flame retardant. With 0.2 ppm antimony is relatively abundant in the earth crust and costs currently 9-10$/kg.[57] Nevertheless, antimony is classified as a critical element by the European Commission.[52] With 80% of the global production volume in 2014, China is the leading global antimony producer. In 2009, China introduced a production quota for antimony, which led to a three-fold price increase by 2011 and caused the flame retardant industry to look for alternatives, leading to a consequent price decline. In 2014 China canceled antimony mining restrictions, as several antimony producers stopped production due to the lack of demand.

Rare earth elements

Rare earth elements comprise a set of 17 relatively abundant elements ranging from cerium with an abundance of 60 ppm to thullium with an abundance of 0.45 ppm, still twice as high as for antimony. Rare earth elements find applications in electric vehicles, wind mills, batteries, mobile phones and television screens. In 2014, China contributed more than 85% to the global rare earth elements production.[58] In 2010, China introduced export quota for rare earth elements, which lead to a sharp price increase, e.g. up to 600% for europium. Early 2015 China canceled the export restrictions, causing the only American rare earth element producer Molycorp to file for bankruptcy. Rare earth elements are classified as critical by the European Commission. Prices vary drastically from element to element.

Zirconium and hafnium

Zirconium and hafnium are byproducts of titanium and tin mining. Hafnium is less abundant than zirconium with a typical ratio of 1:50. The main use of zirconium is to improve the corrosion resistance and thermal cycling stability of alloys, e.g., for chemical piping in corrosive environments or as cladding layer encapsulating nuclear fuel rods to avoid contami-

nation of cooling water with fission fragments. Hafnium is used mainly in turbine blades and in nuclear control rods as the neutron capture cross section of some of its isotopes is high and about 600 times larger than for zirconium. Separating hafnium from zirconium is quite challenging, as both metals have very similar chemical properties. Nevertheless, because of their very opposite neutron capture cross sections, it is mandatory for the nuclear industry to produce hafnium poor zirconium, which leaves hafnium as a byproduct.

There are currently just two major producers of hafnium in the world, ATI Speciality Alloys and Components (fomerly ATI Wah Chang and Teledyne Wah Chang) in the US and Areva in France. The largest production is in Australia followed by South Africa and China. Since 2007 the price of zirconium and hafnium has been rising steadily. Due to the lack of demand following the nuclear reactor melt downs in Fukushima in 2011, the prices did not stop to rise and are currently at 97$/kg and 568$/kg for zirconium and hafnium respectively compared to 32$/kg and 289$/kg back in 2009.[59] Nevertheless the official report on critical raw materials for the EU assess the supply risk for hafnium as relatively small similarly to aluminum and manganese while acknowledging its economic importance.[60] With an abundance of 3.3 ppm per weight in the earth crust, hafnium is actually more abundant than tantalum with 1.7 ppm and tungsten 1.1 ppm.

Consequences for thermoelectrics

The challenge for Bi_2Te_3 thermoelectrics is clearly the price of tellurium of 117 $/kg. Convoluted with the price of Bi of 25 $/kg, Bi_2Te_3 costs about 70 $/kg. In 2011 the council of the European Union extended the exception for CdTe in the restriction on hazardous substances directive[55], so the pressure on the cost of tellurium is not expected to reduce in the near future. With a lead price of 2$/kg and due to the heavy weight of lead, to cost for PbTe is lower 45 $/kg. Nevertheless, the restriction on hazardous substances directive, prohibits the use of PbTe thermoelectrics in Europe.[55]

For skutterudites without rear earth rattlers, the cost for raw materials is relatively cheap at about 13 $/kg. Depending on the filling fraction and the type of rattler, the cost may be significantly higher. All elements in skutterudites are classified as critical by the European commission.

The cost for the base materials of TiNiSn Half-Heuslers is cheap and dominated by the cost of Ni with 17 $/kg or lower, bringing the cost for TiNiSn to about 4-5 $/kg.[61] However, in order to lower the thermal conductivity, Zr and Hf are employed. Zr with a cost of 97$/kg and even more Hf with 568$/kg are prohibitive for thermoelectrics when used in large percentages. Adding 5% of Zr or less than 1% of Hf by weight would already double the cost of the half-Heusler compound. For comparison the $Ti_{0.5}Zr_{0.25}Hf_{0.25}NiSn$ half-Heusler alloy reported by Schwall et al.[30] uses about 8% of Zr and 16% of Hf by weight. The challenge for half-Heusler compounds is therefore to develop materials combination which only use small amounts of these elements. The p-type FeNbSb half-Heusler reported by Fu et al.[34] is a right step in this direction. The price of this compounds is dominated by Nb which costs 42$/kg for ferronobium with 60-70% niobium content.[62]

Magnesium silicides Mg_2Si and tetrahedrites $Cu_{12}Sb_4S_{13}$ offer both a very advantageous cost structures. All constituent elements cost less than 1$/kg and none of the elements is critical. One caveat is that the amount of Ge in Mg_2Si must be kept as low as possible as Ge costs up to 1900 $/kg depending on quality. N-type Mg_2Si and p-type $Cu_{12}Sb_4S_{13}$ can be integrated together into a thermoelectric module as the example of Alphabet Energy shows, which recently adopted these two materials for their products.[63]

2.5 Mechanical and thermal stability of thermoelectrics

Very little information on the mechanical stability of the different thermoelectric material classes is available from literature. The mechanical properties of the sintered materials strongly depend on the density of the sintered bodies. Also very poorly documented in litera-

ture are phenomena associated with mechanical fatigue and degradation of electronic properties of thermoelectric materials upon thermal cycling as well as the mechanical and thermal stability of contact and diffusion layers. More work in this direction is needed in particular when considering thermoelectrics for non-stationary applications where the impact of shocks and vibrations and thermal cycles may be high.

2.6 Reliability and relevance of thermoelectric transport data

The photovoltaic community has been employing standardized measurement protocols for many years enabling direct comparison between results in terms of power conversion efficiency as well as other performance indicators. Record efficiencies must be certified independently by accredited measurement groups and are reviewed by an international panel of experts in the field before they can enter the official record tables published biannually in a scientific journal and online.[64,65] In order to improve reproducibility and transparency of published data, one of the most prestigious journals recently even introduced a 'reporting checklist' where authors of scientific publications are required to disclose details on the fabrication and measurement procedures.[66] These measures have contributed to considerably reduce the number of announcements of unsubstantiated breakthroughs and record efficiencies.

The thermoelectric community has not yet reached a comparable of level maturity due to the complexity of determining the figure of merit zT. The International Energy Agency, under the implementing agreement for Advanced Materials for Transportation, has recently conducted international round robin tests, with the intention to foster the development of international test standards, improved test methods, and better characterization tools.[67,68] These studies have shown that even routine measurements conducted by experienced groups may lead to differences in zT of up to 20%, with a general trend to larger uncertainties with increasing temperature. The determination of the heat capacity required to determine the thermal conductivity from the thermal diffusivity represents the largest contribution to the error,

but also systematic differences due to different measurement geometries and protocols can add an error to the Seebeck coefficient on the order of 5%. An overview of measurement techniques required for the determination of zT and their inherent difficulties has recently been given in Ref. 69. There are currently no official record tables for thermoelectrics and claims of extraordinarily high zT values may often be the result of incorrect measurements. A large spread in zT values may be the result of bad contacts, inhomogeneities, chemically reacted or cracked samples, or wrong calibration.

Not only measurements should be repeatable, but also the synthesis routes. However, very often crucial details on sample preparation are missing in literature. While sample stoichiometries are relatively well reported and synthesis procedures are typically relatively well reported, it is striking that e.g. details on the (ball) milling and (hot press or spark plasma) sintering conditions are almost never specified. Taking into account that much of the advances of the thermoelectric field in recent years were related to the modification of a polycrystalline thermoelectric raw material into a densely sintered nanobulk form, more stringent reporting requirements would be highly desirable.

It was pointed out again only recently that the formula given on page 7 to determine the maximum efficiency of a thermoelectric material based on its zT values is only valid in the limit of constant physical properties. Practically this means that the formula is only useful for small temperature differences, where this assumption becomes valid. To avoid solving complex differential equations, a relationship between zT and the maximum conversion efficiency was given in terms of a combination of integrals over the temperature dependent physical properties of thermoelectric materials.[8] This theoretical framework we applied in this work to determine the maximum efficiencies of best-in-class thermoelectric materials in Fig. 1, 2, 3, and 4.

It is important to realize that the maximum efficiency at a given hot side temperature and cold side temperature determined from the zT values of a thermoelectric material does not

represent a system efficiency. Suboptimal compatibility between n-type and p-type thermoelectric materials, electrical contact resistances at the module level, and thermal contact resistances at the module but also system level including the heat exchangers on the cold and hot side will all contribute to reduce the efficiency of the overall system. In the recently completed CCEM and OFEN co-funded project HITTEC, improvements in contact resistance led to an increase of the output current density by more than a factor of 2. Nevertheless, while the modules performed very well on a thermoelectric module test rig (output power density of 640 mW/cm^2 at a temperature difference of 800°C), the power output on the system level (6 mW/cm^2) remained far below expectations due to the low temperature difference (70°C) and low heat flux across the module[70]. This example emphasizes the importance of a careful thermal design at the system level.

3. Assessment of industrial waste heat potential

The following information about the potential of industrial waste heat for the application of thermoelectric generators derives from Ref. 71.

3.1 Industries with waste heat potential

As there is no data on industrial waste heat in Switzerland available, we take the energy intensity on industry level as an indicator. The energy consumption per production site is calculated to give an idea of the potential of waste heat. This indicator clearly shows that the chemistry/pharmaceutical industry, cement/concrete production and metal/steel production industries have the greatest potential. The next-largest potential lies in food production. This potential may actually be larger than shown by the indicator, as the industry itself is very heterogeneous when it comes to plant size. It is therefore plausible that a non-negligible number of very large waste heat producers exist in the food production industry.

Table 1: Energy consumption and structure of the relevant industries 2012 - Switzerland. Source: SFOE

Energy statistics 2012	Total TJ	Production sites (PS)	FTE	TJ/PS	GWh/PS
Cement / Concrete	13'941	38	1'595	366.87	101.91
Metal / Steel	7'496	124	7'563	60.45	16.80
Chemistry / Pharmaceutical	32'198	822	59'202	39.17	10.88
Food	17'070	2'521	54'389	6.77	1.88
Paper / Printing	12'985	2'524	29'941	5.14	1.43
Metal Devices	15'758	10'174	200'872	1.55	0.43

3.2 Industries with cold water potential

As also calculated and shown for the calculation of the potential for the magnetocaloric machine for power generation a cold as well as a hot medium is needed for the thermoelectrical modules. Therefore we looked at the availability of cold and hot water in industry. The following information about the water potential derives from the Ref. 71.

Water data is partially available locally and for the cantons, but are not publicly accessible. Based on our knowledge, the newest and only statistic for water use by the industry comes from 2009, written by the Swiss Association for Gas and Water (SVGW). The data relate to the operating year 2006. Not all industry branches are recorded in the statistics, the relevant water users can however be displayed representatively.

The SVGW statistics (2009) clearly show that the largest users are nuclear power plants, followed by the industrial sector (see Fig. 6). Relevant industries for water use are the chemical, waste, paper, metal and food industries (see Fig. 7). How much of this water can be used as waste heat or cold sources is not apparent from this data and had to be clarified individually.

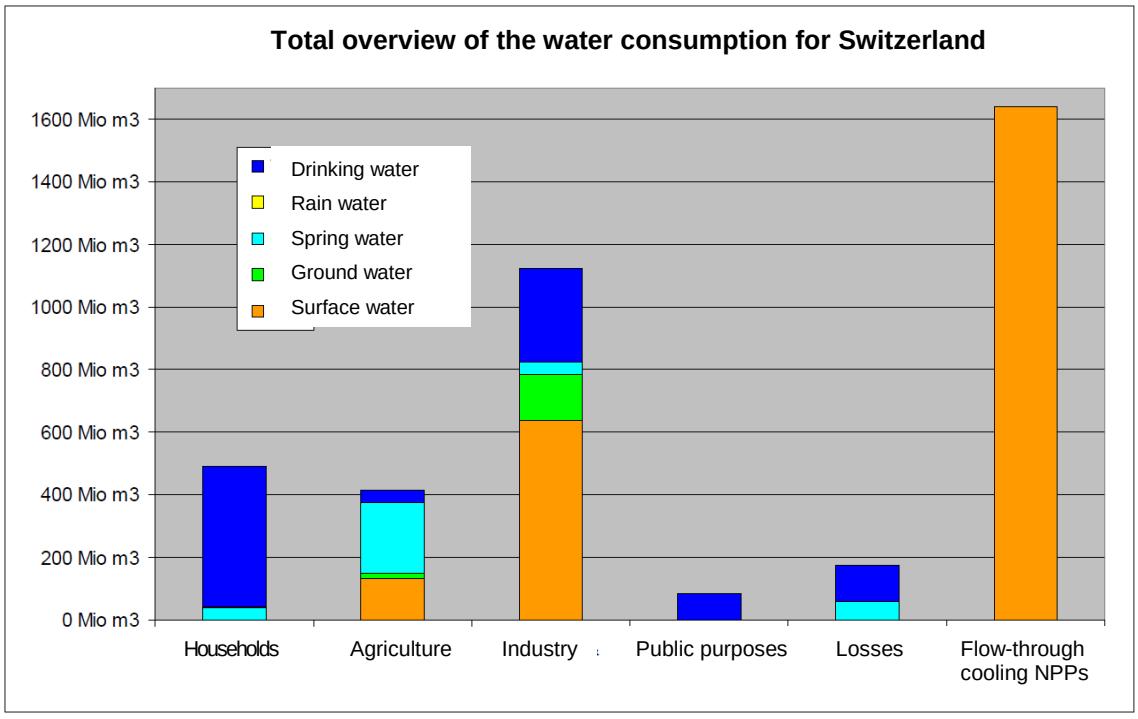

Fig. 6: Total overview of the water consumption for Switzerland in 2006. Source: SVGW (2009)

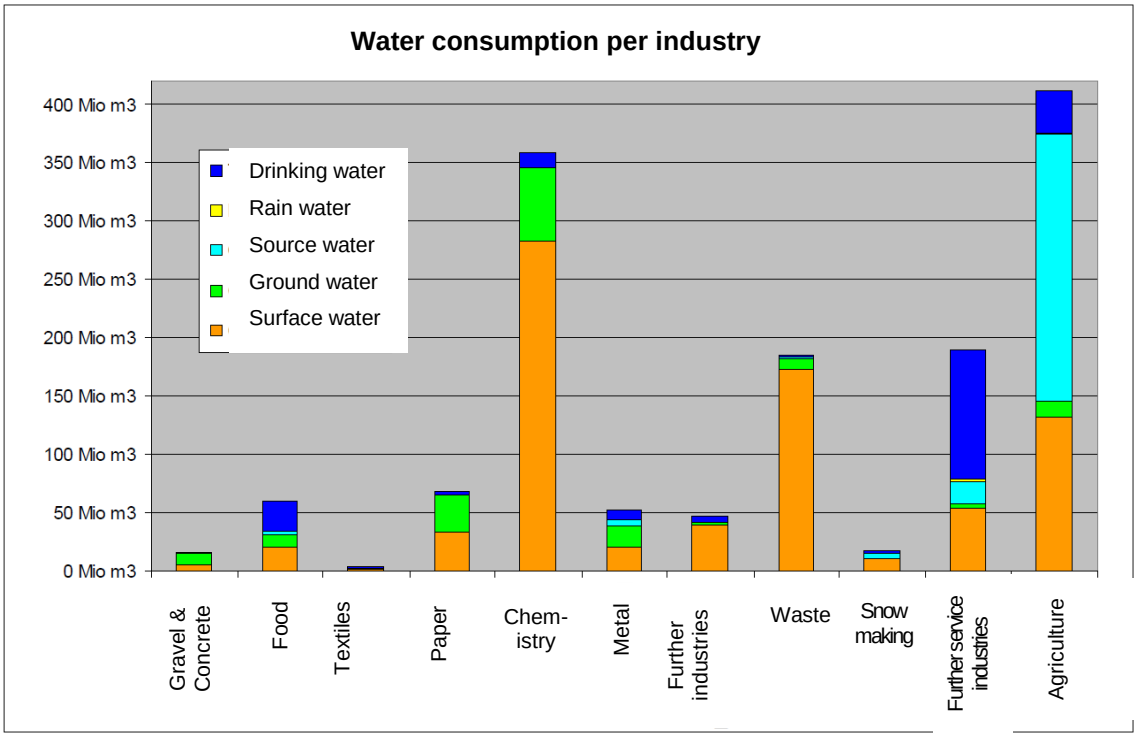

Figure 7: Water consumption per industry in 2006. Source: SVGW (2009)

3.3 Industries with waste heat and cold water potential

From this analysis, we conclude that the branches of chemical, metal, paper and food industry could be potential sites for thermoelectric energy recovery. Aside from the paper industry, partners for relevant business cases were found in all industry branches. However, the production processes within the branches are very heterogeneous, making generalization of the results complicated. Additionally, the cement and concrete industry were investigated due to the high energy demand per working site and the relatively standardized production process.

3.4 Industries with waste heat at a temperature of 250°C

To investigate the estimated potential of waste heat in the 250°C temperature range, interviews were conducted with company representatives and supplemented by research data. From the four companies studied, it would appear that either waste heat in the 250°C temperature range is already used, concentrating the waste heat would be too laborious, or the process

heat is already employed for other internal processes (for details see Appendix).

A study published by the Swiss Federal Office of Energy in 2011 also indicates that industrial waste heat is mainly generated at low temperatures between 30 and 40°C.[72] Central or local heat pumps can be used to raise the waste heat to a higher, usable temperature.

We can conclude that the potential for industrial waste heat in the 250°C temperature range is very limited in Switzerland and focused on companies using waste heat in the 65°C temperature range.

4. Processes competing with thermoelectrics by temperature range

4.1 Temperature range between 350°C and 650°C

In Switzerland, process heat in the temperature range between 350°C and 650°C is generated mainly from the following industries or power generation plant technologies:

- Cement industry
- Glass manufacturing
- Brick works
- Waste incineration plants
- Special waste incineration plants
- Old wood incineration plants
- Forest wood incineration plants

Table 2 summarizes the standard techniques for the utilization of process heat as well as potential alternative techniques. These include the classic water steam-cycle (in which heat is transformed to electric power with a turbine), the organic Rankine cycles (which uses an organic liquid instead of water) and transfer of surplus heat produced during the process at a high temperature level to a remote location, where heat can be used at a lower temperature level. Organic Rankine cycle technology is already established in particular for biomass plants but also in the cement production plant in Wildegg AG and Untervaz GR. The organic Rankine cycle represents a direct competitor for thermoelectric generators.

Table 2: Utilization of process heat in typical Swiss industries in high temperature segment.

Industry or power plant technology	Standard utilization	Potential alternative utilization
Cement industry	Transfer of heat to preheat raw material	Conversion of heat to electric power via organic Rankine cycle
Glas manufacturing	Transfer of heat to preheat combustion air	
Brick manufacturing		
Waste incineration plants	Conversion of combustion heat to electric power via water steam cycles, heat transfer into water steam-cycle, heat transfer to remote heat network	In various incineration plants exists still potential for heat transfer and/or conversion to electric power via organic Rankine cycle
Special waste incineration plants	Conversion of combustion heat to electric power via water steam cycles, heat transfer into water steam cycles, heat transfer to nearby processes	Special waste incinerators are small in Switzerland and integrated into industrial chemical plants, remaining potential is utilized by heat transfer processes
Old and forest wood incineration and biomass power plants	Conversion of combustion heat to electric power via water steam or organic Rankine cycles (>50%), condensation heat is used to dry wood or transferred to remote heat networks	As for waste incineration plants

4.2 Temperature range between 250°C and 350°C

In the temperature range between 250°C and 350°C, the chemical industry and paper factories need to be considered in addition to the industries listed in 4.1. In this temperature range, heat from exothermal processes in the chemical industry can be used to produce saturated vapor that can be supplied directly to generate heat for endothermal processes. In the paper industry, heat transfer processes can be used for drying purposes. The integration of a thermoelectric generator would hinder the heat transfer and consequently reduce the efficiency of the subsequent process. The application of a thermoelectric generator in this temperature range is therefore thermodynamically not recommended. The potential for increasing the energy efficiency of systems by heat transfer can be determined using a pinch analysis.

4.3 Temperature range between 120°C and 250°C

In this temperature range, heat is transported by wet steam or hot water even over long distances. Heat can therefore be supplied to remote locations in industrial settings but also to supply hospitals with heat at a lower temperature, e.g. Wärmeverbund Rheinsalinen Ost[73]. Remote heat in this temperature range replaces heat generation through the combustion of fossil energy carriers and contributes significantly to the reduction of CO_2 emissions. Thermoelectric generators from these sources would be counter-productive to this reduction of CO_2 emissions.

The generation of electric power via a thermoelectric generator, which could be built into the heat exchanger responsible for remote heat generation, would lead to a reduction in the generation of remote heat and consequently increased CO_2 emissions. Thus with respect to minimizing CO_2 emissions, the use of thermoelectric generators in this temperature range is not suitable.

Table 3: Ecological comparison of process heat utilization by CO_2 emission reduction

	Thermal to thermal efficiency [%]	**Thermal to electric efficiency [%]**	**CO_2 reduction according to Swiss CO_2 legislation [%]**	**CO_2 reduction according to KBOB[a] for Switzerland [kg CO_2/kWh]**
Heat transfer	85-95	-	85-95	0.237[b]
Remote heat network	85	-	85	0.237[b]
Water steam cycle	-	23-29	0	0.030[c]
Thermoelectric conversion	-	2.5	0	0.030[c]

[a] based on values from list 2009-1 of the Koordinationskonferenz der Bau- und Liegenschaftsorgane der öffentlichen Bauherren (KBOB)
[b] replacing heat generation by natural gas
[c] replacing electricity by electricity from the Swiss grid

From an economic point of view, similar conclusions can be drawn. The financial payback time of heat transfer approaches is typically in the range of 5 years and realized by industry. Investments into remote heat networks are economically questionable. The conversion of heat into electric power via water steam cycles in e.g. waste incineration plants requires subsidies in order to justify investments in further power extensions with thermoelectric generators.

Table 4: Economic comparison of process heat utilization

	Accepted payback time in years
Heat transfer	5
Remote heat network	10
Water-steam / organic Rankine cycle	10
Thermoelectric conversion	> 10

Nevertheless, there are process areas in waste incineration plants, where the heat of the exhaust gas stream remains unused and is released to the environment. These areas are investigated in chapter 5.

4.4 Temperature range between 65°C and 120°C

Similar considerations as for remote heat networks discussed in 4.3 apply also for the temperature range between 65°C and 95°C. Process heat from industrial cooling circuits may amongst other possibilities be transferred to locations where heat is needed, e.g. for warm water supply and heating in building or heat generation for low temperature processes. Companies employing this approach include Kabelwerke Brugg AG and Victorinox Ibach SZ[74]. In waste incineration plants heat contained in exhaust gases released through the chimney may be converted via organic Rankine cycles or thermoelectrics (see chapter 5).

4.5 Organic Rankine cycles

In the temperature range between 250°C and 650°C organic Rankine and water-steam cycles compete with thermoelectric generators. Organic Rankine cycles are processes in which analogously to the water steam cycle, an organic fluid evaporates upon absorption of process heat and is expanded in a turbine. The mechanical power of the turbine is transformed into electric power via a generator. Contrary to water steam cycles, organic Rankine cycles exhibit a high efficiency also at process temperatures below 350°C, approaching the ideal Carnot process. Infrastructure for organic Rankine cycles is very compact, requires relatively

small investments, is practically maintenance free, and can be installed rapidly. Electrical power output is currently in the range of 10 to 1'500 kW. Nowadays in small power plants, such as biomass power plants, organic Rankine cycles are preferred over water steam cycles.

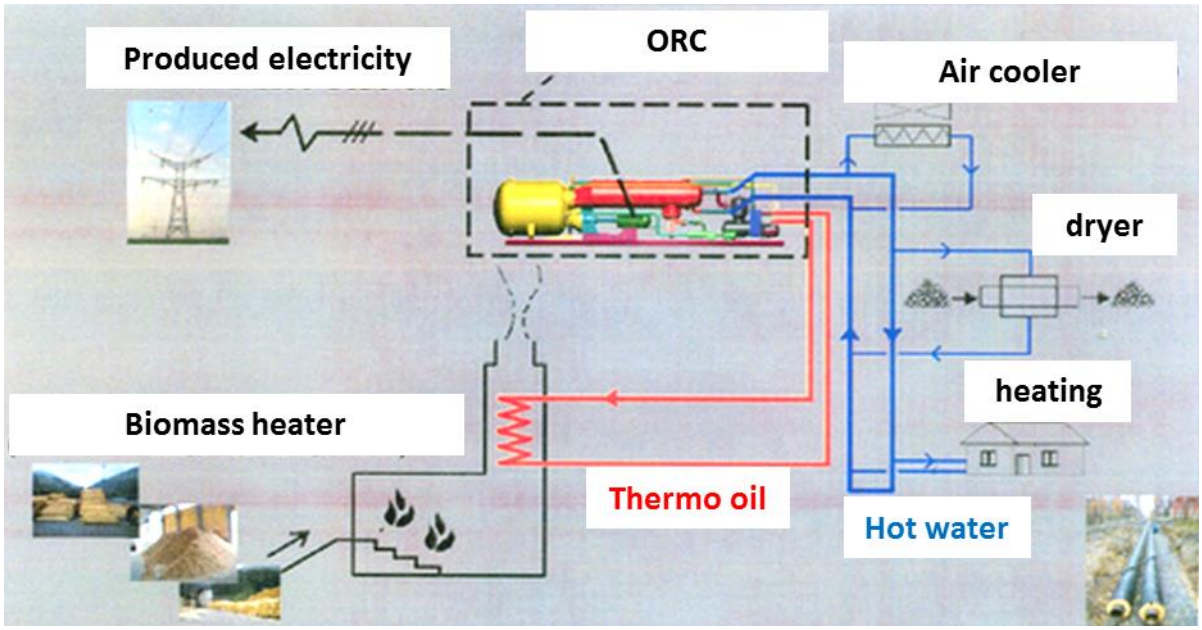

Figure 8: Principle of operation of the biomass plant in Nesslau SG

The heat conversion efficiency of an organic Rankine cycle ranging from 12% at low temperature to about 18% at high temperature exceeds a thermoelectric generator with an assumed efficiency of about 2.5%. From a technical point of view, thermoelectric generators consequently do not represent a viable alternative to organic Rankine cycles at these temperatures.

Table 5: Comparison between the Carnot power conversion efficiency with the power conversion efficiency of the organic Rankine cycle at the biomass plant Nesslau SG.

Hot side temperature [°C]	Cold side temperature [°C]	Carnot efficiency [%]	Efficiency of the organic Rankine cycle [%]
290	180	20	18
260	180	15	14

Reducing the hot side temperature of the organic Rankine cycle from 290°C to 260°C reduces its total efficiency by 4% (see table 5). Consequently putting a thermoelectric generator in series with the organic Rankine cycles does not make sense, as the reduced efficiency of the organic Rankine cycle cannot be compensated by the additional electrical output power from the thermoelectric generator, assumed to be 2.5%.

Table 6 shows the application of organic Rankine cycle processes in wood combustion plants in Switzerland. Organic Rankine cycle processes therefore are the process of choice within the temperature range above 250°C.

Table 6: Overview of biomass power plants in Switzerland using organic Rankine cycles.

Location	Installation	Status	Production	Energy carrier	Electric power [kW]	ORC supplier
Bière VD	1998	op.	CHP	biomass	335	Turboden
Crissier VD	2002	op.	CHP	biomass	500	Turboden
Gossau SG	2010	op.	CHP	biomass	1000	Turboden
Nesslau SG	2010	op.	CHP	biomass	500	Adoratec
Bichelsee-Balterswil TG	2010	op.	CHP	biomass	610	Turboden
Wittenbach SG		u.c.	CHP	biomass	600	Turboden
Speicher AR		u.c.	CHP	biomass	610	Turboden
Ilanz GR		u.c.	CHP	biomass	350	
Lausanne VD	2010	op.	CHP	remote heat		Eneftech
Klingnau AG	2013	op.	CHP	heat biogas engine	30	Eneftech
Lignerolle VD	2014	op.	CHP		30	Eneftech

"op." = Operational systems
"u.c." = Systems under construction
"CHP" = combined heat and power

The following paragraph is considering the necessary investment for an organic Rankine cycle system. Table 7 presents a cost estimation for a system that transforms heat from hot exhaust gases of a waste incineration plant in front of the chimney at a hot side temperature of 120°C. This case is not optimal for an organic Rankine system. The goal of the calculated cost estimation is the determination of the threshold for economic viability. For a 560 kW system,

the target price is CHF 5446. According to the calculations presented in section 6 of this report, this represents a positive business case.

Table 7: Investment costs for organic Rankine cycle systems with different output power level

Transferred thermal power [$MW_{thermal}$]	**1.0**	**2.0**	**4.0**
Electric power output [MW_{el}] by η = 14%	0.14	0.28	0.56
Investment position	Costs [CHF]		
ORC setup	600‘000	900‘000	1‘100‘000
Cost of heat exchanger[a]	100‘000	150‘000	225‘000
Cost for ORC condensator	200‘000	300‘000	450‘000
Cost for heat tubings[b]	50‘000	75‘000	100‘000
Electrical cables and connectors	50‘000	75‘000	100‘000
Mechanical installation	300‘000	450‘000	675‘000
Rubber for chimney	200‘000	200‘000	200‘000
Engineering	200‘000	200‘000	200‘000
Total costs	**1‘700‘000**	**2‘350‘000**	**3‘050‘000**

[a] A gas-water heat exchanger is assumed here.

[b] Assuming a tube length of 50 m for forward and backward piping at CHF 500/m

Table 7 shows a clear economy of scale: by duplication of transferred thermal power the total costs increase less than proportional.

4.6 Conclusions on potential applications of thermoelectrics

In the range above 65°C, thermoelectric heat to electricity conversion competes directly with heat transfer, remote heat utilization, or water steam and organic Rankine cycles. Due to the relatively low conversion efficiency of thermoelectric generators (2.5%) their use is only in exceptional cases ecologically appropriate and economically viable.

In the temperature range below 65°C exists a huge opportunity for thermoelectrics as the conversion efficiencies of cycle processes become low. In addition, cycle processes are relatively complex and not always compatible for refurbishing existing infrastructure and certainly not suitable for upgrading heat pumps in industrial manufacturing.

5. Identification of technical opportunities for thermoelectrics

Based on the conclusions drawn in section 4.6, the following potential applications for thermoelectrics are identified:

- Applications in special cases of thermal processes
- Heat to electricity conversion during condensation in water steam or organic Rankine cycles
- Heat to electricity conversion in cooling cycles powered by heat pumps

5.1. Applications in special cases of thermal processes

In the extensive survey "Analysis of potential to increase the electricity generation of waste incinerators"[75] all of the 28 Swiss waste incineration plants have been investigated with respect to their potential for further process and waste heat utilization. Based on the energy flow diagram of Swiss waste incineration plants (see Fig. 9), additional potential to reduce heat losses through heat to electricity conversion exists at the level of steam processes through condensation and exhaust gases. Based on this overview, the potential for further heat to electricity conversion in a standard Swiss waste incineration plant was investigated.

In the high temperature range, two areas with potential for heat to electricity conversion are identified:

- between electrostatic precipitator and quench
- along the exhaust chimney

As the temperature in these locations is too high for direct injection into an organic Rankine cycle, exhaust gases are cooled down via a water/thermo-oil heat exchanger, which could be equipped with thermoelectric generators. Assuming a thermoelectric conversion efficiency of 2.5%, the overall efficiency of thermoelectric combined with organic Rankine cycle would not really be higher than of the organic Rankine cycle alone. Therefore the combination of thermoelectric generators and organic Rankine cycles should not be followed as long as the

efficiency of thermoelectric is below 5%. In the low temperature range, waste heat may be utilized via condensation.

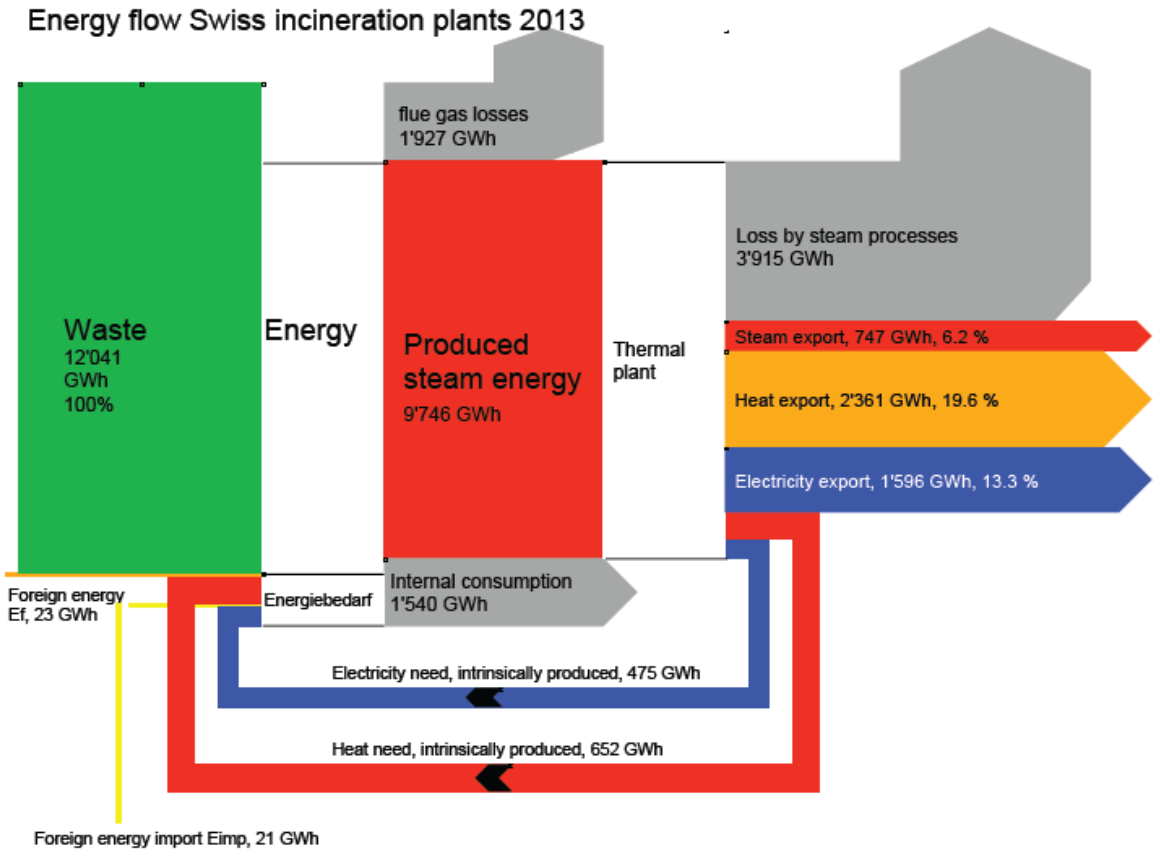

Fig. 9: Energy flow diagram of all Swiss incineration plants

5.2. Integration of thermoelectrics into condensation zone of waste incineration plant

For the integration of a thermoelectric generator into the condensation zone of a waste incineration plant, a plate heat exchanger needs to be installed as the thermoelectric generators cannot be mounted easily on the tubes of the condenser. This arrangement requires careful optimization.

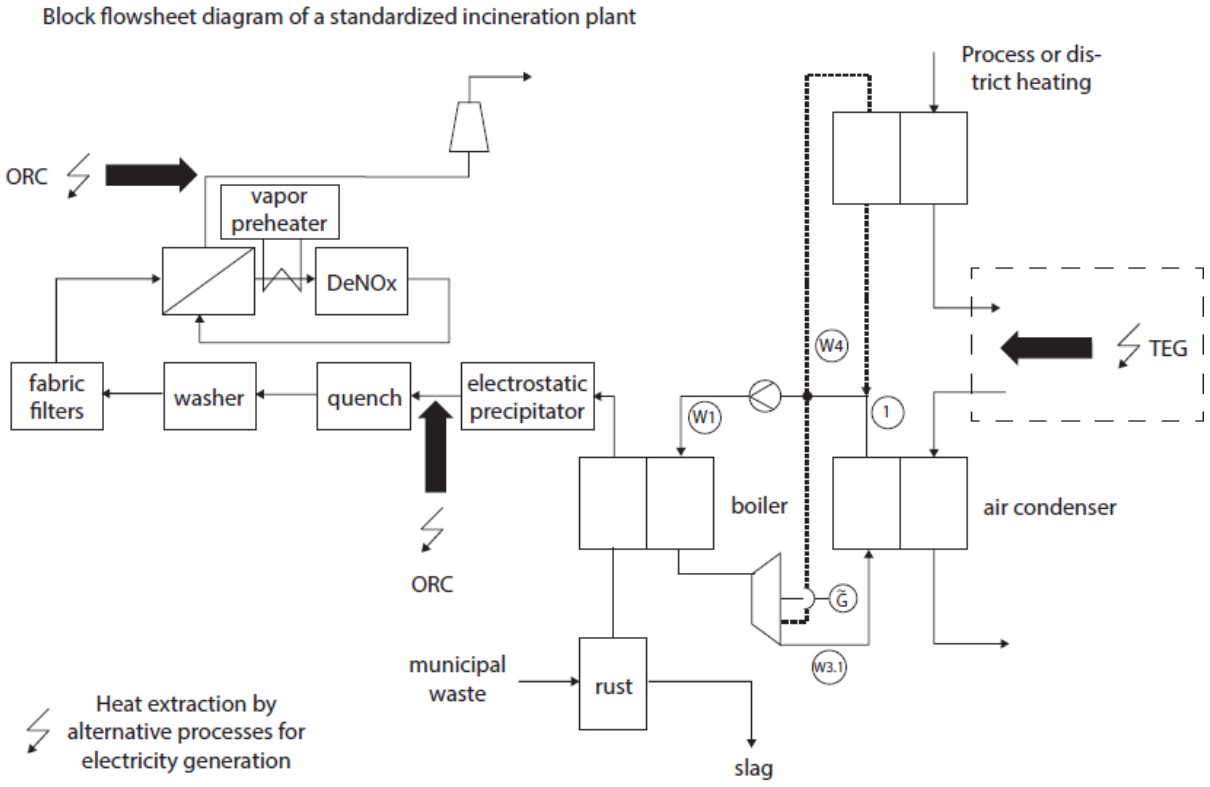

Figure 10: Flow diagram of a typical incineration power plant

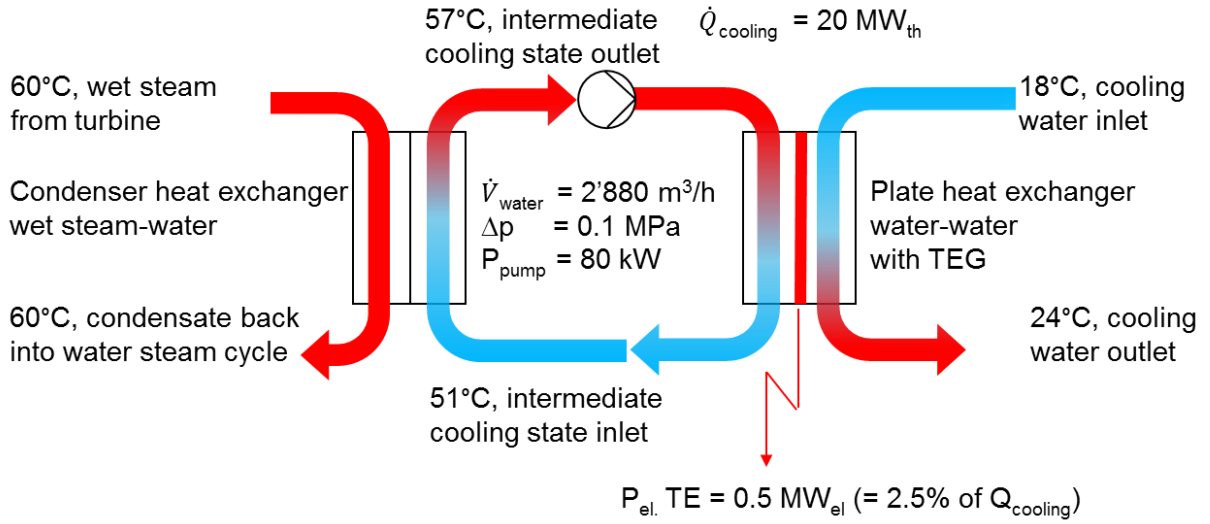

Figure 11: Schematic of integration of a thermoelectric generator in the condensation zone of a water steam cycle of a waste incineration plant

5.3 Cumulated potential for heat to electricity conversion of all 28 Swiss waste incineration plants

In the extensive survey "Analysis of potential to increase the electricity generation of waste incinerators"[75] all of the 28 Swiss waste incineration plants have been investigated with respect to their potential for their heat to electricity conversion following the approaches described in 5.1, 5.2 and 5.3. In this assessment a thermoelectric power conversion efficiency of 2.5% was assumed in the low temperature range. Thermoelectric generators could be considered within the condensation process when condensation takes place at temperatures above 60°C.

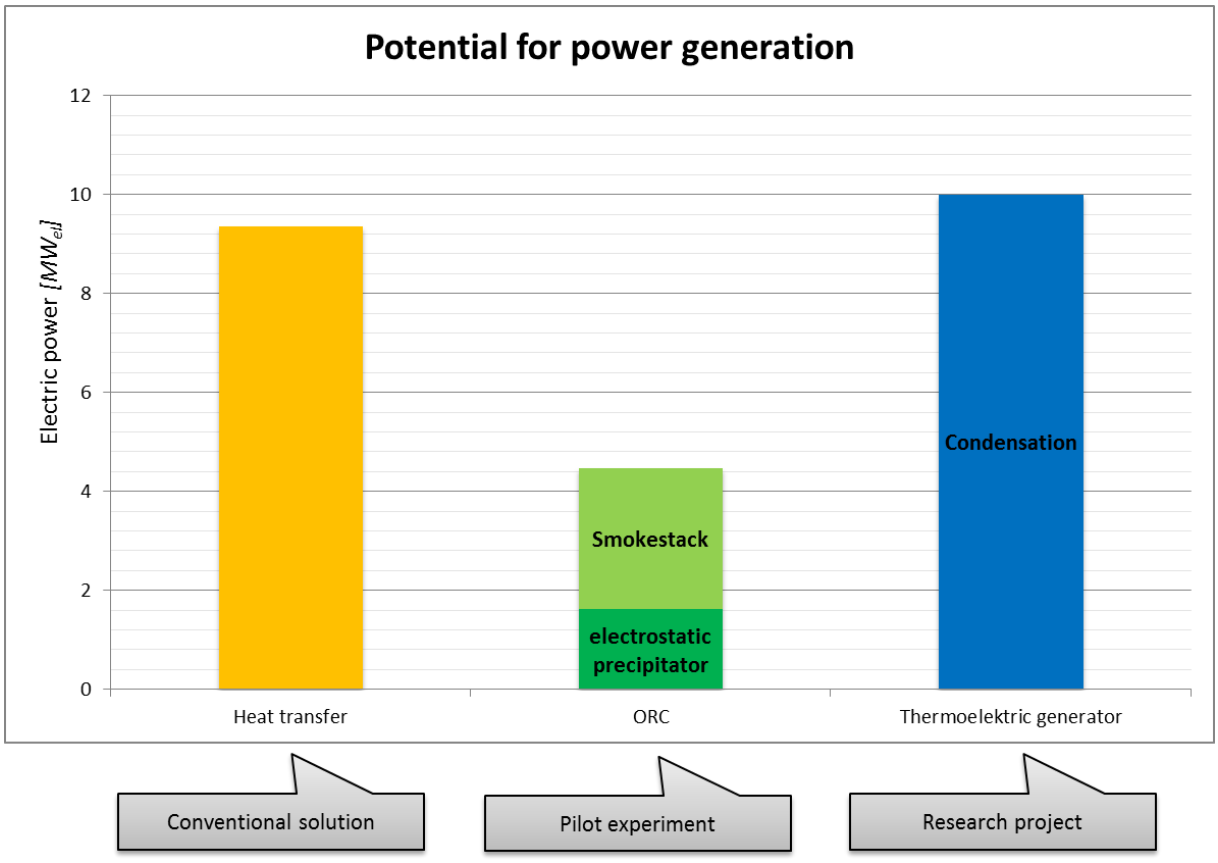

Figure 12: Cumulated potential for heat to electricity conversion in the 28 Swiss waste incineration plants

Of particular interest are cooling processes for which ground-, river- and lake water is used.

6. Economic feasibility of industrial waste heat recovery market

6.1. Calculation of the target price

The following business cases stem from the metal/steel, energy production, food, cement, and chemical/pharmaceutical industries. All cases were made with Swiss companies. The market segments are divided according to available mass flows. If more than 50m^3/h of hot and cold water respectively are available, the company is classified as a large waste heat producer. The target price is the maximum accepted market price for a thermoelectric technology. This price contains a profit margin aimed for by the manufacturer along with the production and installation costs. Operational, technical and economic factors are considered in the calculation. The target price was calculated as follows:

$$Target\ Price = \sum_{t=1}^{T} \frac{CF_t}{(1+i)^t}$$

- $CF_t = E_t - A_t$
- $E_t = Price_{el} * operating\ hours * P_{el.TE_{net}}$
- $A_t = [Price_H * \dot{m}_H + Price_C * \dot{m}_C + Price_{el}(P_{net_{pumpH}} + P_{net_{pumpC}})] * operating\ hours + K_{maintainance}$

$H \dots warm\ medium$

$C \dots cold\ medium$

$P \dots performance$

$\dot{m} \dots mass\ flow$

$Price_{el} \dots Price\ electric\ power$

$K \dots costs$

The analysis below suggests an average target price per kW installed power of 3'000 CHF which can be considered the maximum sales price per kW of thermoelectric technology for waste heat recovery.

Table 8: Target Price for 5 cases

		Unit	Case 1: Food industry	Case 2: Cement industry	Case 3: Metal/steel industry	Case 4: Chemical industry	Case 5: waste incineration plant
Volume	WW	m^3/h	60	130	25	10	2'880
	KW	m^3/h	60	130	25	10	
Temperature	WW	°C	28	60	40	60	54
	KW	°C	6	25	15	13	21
Price / Costs	WW	CHF/m^3	0	0.00	0	0	0
	KW	CHF/m^3	0	0.00	0	0	0
	Elec-tricity	CHF/kWh	0.11	0.10	0.12	0.10	0.05
Operating hours		h/a	8’760	7'000	7'600	8'400	8'000
Payback period		a	5	5	5	5	10
Interest rate		%	8	8	8	8	8
Thermic efficiency		%	2.5%	2.5%	2.5%	2.5%	2.5%
TE power		kW	38	132	18	14	2'760
Pump power		kW	10	2.5	0.5	0.2	114
TE net power		**kW**	**28**	**130**	**18**	**14**	**2600**
Net production MWh		MWh/a	248	907	134	113	21'172
Target Price / kW (electrical)		**CHF/kW**	**2‘900**	**2‘700**	**3‘500**	**3‘300**	**2'500**
Target Price Total		**CHF**	**109‘000**	**359‘000**	**64‘000**	**45‘000**	**6'949'000**

6.2 Sensitivity analysis

In order to better understand the relevance of the different input values on the target price, a sensitivity analysis was conducted in this section. A standardized comparison between the input values was made.

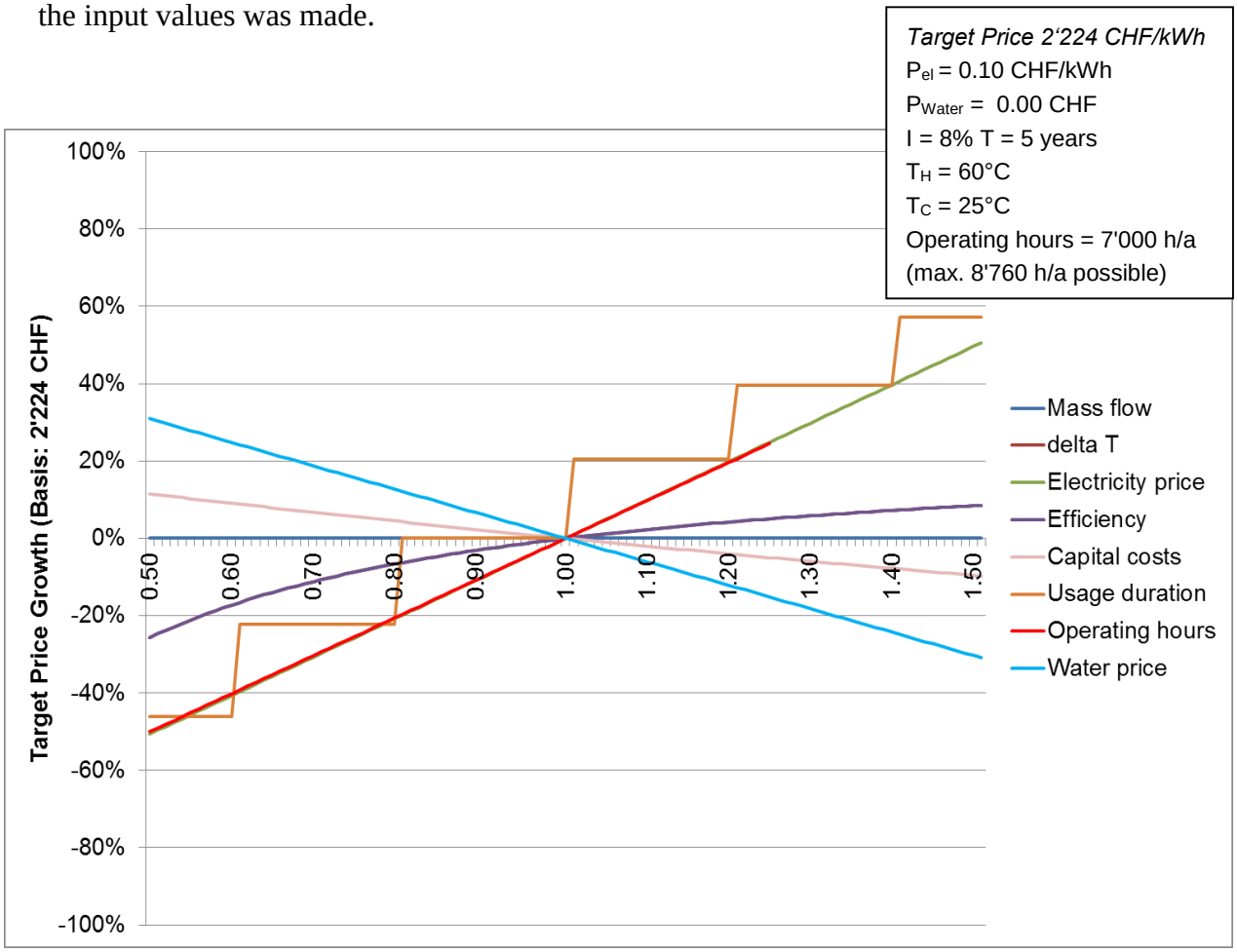

Figure 13: Sensitivity analysis for target price

Fig. 13 shows the comparison of all input values on the target price per kW installed power. The horizontal axis shows the standardized variation of the input values, the vertical axis shows the growth of the target price. Using the example of the price of electricity, a 50 % higher price of electricity (from index 100 to 150) would cause a growth of the target price of 50%. Or a 50% higher thermal efficiency would allow a 10% more expensive machine.

The duration of use, the electricity and water price have the strongest impacts on the profitability. The operating hours would have the same potential as the electricity price if they were not naturally limited. The second most important influence factors are the capital costs

and the efficiency. The mass flow has no influence, since the cash flow grows proportionally to the power increase.

The efficiency of the machine therefore have a much smaller influence on the profitability than economic values, however they may be directly influenced. The price of electricity and cost of capital are given by the market. The price of water is either provided by the regulator or is defined via the operating costs (e.g. cooling tower). Here, it is important to identify innovative concepts for the integration into processes in order to keep the costs low (e.g. recycling of cooling water). Simultaneously, the available ΔT and the mass flow may be optimized. The efficiency and the operating hours can be increased by technical developments, contrary to the other factors. A small maintenance window and a high reliability increase the operating hours.

6.3 Market potential estimation

The model for the market potential estimation is based on a model developed for magneto-caloric machines.[71] Similar to the magneto-caloric effect thermoelectric is based on a temperature difference and therefore a usable hot and cold water source must be available. Contrary to the magneto-caloric technology however thermoelectric is also feasible for relatively small volume flows. The market potential estimation for thermoelectric is therefore based on the used primary energy per industry, independent of the size of the production sites (exception: very small companies with too less waste heat).

The estimation of the market potential is using the same assumptions as used for the magneto-caloric machine[71] as long as these assumptions are reasonable from a technical point of view. This approach allows for comparable market size estimations for these two competing technologies of waste energy use. Furthermore, we assume that 80% of the used primary energy is available in form of waste heat and is produced on average during 7'500 hours per year. The market potential (in CHF) for thermoelectric units was calculated with an average

sales price of 3'000 CHF/kW (compare section 6.1.).

As expected the market potential for thermoelectric heat units is about 5 times higher than the market potential for magneto-caloric machines. This is due to the more flexible application also in mid-size and smaller production sites.

Industry			Market potential					
	TJ/industry (MSW MW)	GWh/industry	Reduction factor "cold water available"	Reduction factor "too small for relevant waste heat"	Available waste heat (kWh)		Market potential (number of kW-units)	Total market potential (in CHF)
			50%		80%	7500	3%	3000
					% Waste heat	Operating hours		Target Price (CHF/kW)
Switzerland								
Industrial Processes	(BFE, Endenergieverbrauch Industrie 2011; Tabelle 4; S15)		(Helbling et all; 2014)	Estimation	(Helbling et all; 2014)			Average Target Price Cap. 5.1
Chemistry / Pharmaceutical	32198	8900	50%	20%	80%	380000	11000	33000000
Metal / Steel	7496	2100	50%	10%	80%	101000	3000	9000000
Metal devices	7496	2100	50%	60%	80%	45000	1000	3000000
Paper / Printing	12985	3600	50%	80%	80%	38000	1000	3000000
Cement / Concrete	13941	3900	50%	20%	80%	166000	5000	15000000
		Compare Cap. 2: 20 MW						
Solid waste incinerater MSW		150.0	50%	0%		10000	300	900000
Total Switzerland							**21'300**	**63'900'000**

Table 8: Market potential estimation for Switzerland

Table 9: Market potential estimation for Germany

Industry			Market potential					
	GJ	GWh	Reduction factor "cold water available"	Reduction factor "too small for relevant waste heat"	Available waste heat (kWh)		Market potential (number of kW-units)	Total market potential (in CHF)
		0,0002777778			80%	7500	3%	3000
	https://www.uid.admin.ch/Search.aspx				% Waste heat	Operating hours		Target Price (CHF/kW)
Germany								
Industrial Processes			(Helbling et all; 2014)	Estimation	(Helbling et all; 2014)			Average Target Price Cap. X
Metallerzeugung und -bearbeitung	919702823	255500	50%	20%	80%	10901000	327000	981000000
Herstellung von chemischen Erzeugnissen	1279166078	355300	50%	10%	80%	17054000	512000	1536000000
Herstellung von Papier, Pappe und Waren daraus	270812005	75200	50%	30%	80%	2807000	84000	252000000
Herstellung von Glas, -waren, Keramik, Verarbeitung von Steinen und Erden	277971017	77200	50%	20%	80%	3294000	99000	297000000
Herstellung von pharmazeutischen Erzeugnissen	25262170	7000	50%	20%	80%	299000	9000	27000000
Getränkeherstellung	24651658	6800	50%	40%	80%	218000	7000	21000000
Herstellung von Nahrungs- und Futtermitteln	200663472	55700	50%	40%	80%	1782000	53000	159000000
Herstellung von Gummi- und Kunststoffwaren	82465171	22900	50%	40%	80%	733000	22000	66000000
Herstellung von Druckerzeugnissen, Vervielfältigung von Ton-,	21039899	5800	50%	40%	80%	186000	6000	18000000
Gewinnung von Steinen und Erden, sonstiger Bergbau	14695036	4100	50%	40%	80%	131000	4000	12000000
Herstellung von Metallerzeugnissen	95808420	26600	50%	40%	80%	851000	26000	78000000
Total Germany							**1'149'000**	**3'447'000'000**

6.4 CO_2 saving potential

The CO_2 saving potential is calculated on the basis of the market potential estimation

presented in the previous section 6.3 (number of potentially installed units multiplied by average operating hours and the relevant CO_2/kWh-conversion factor by country). The official conversion factor of the Swiss suppliers electricity mix provided by SFOE (2014) of 122 g CO_2/kWh was used as conversion factor. This factor is 558 g CO_2/kWh for Germany[76]

Table 10: CO_2 saving potential with thermoelectrics

	Switzerland	Germany
CO_2 theoretical saving potential	approx. 19'000 t	approx. 4.8 Mio. t
$C0_2$ saving potential based on 10% market penetration	approx. 2'000 t	approx. 480'000 t
Total emissions 2013	approx. 57 Mio. t	approx. 820 Mio. t

6.5 Production costs

To fully assess the potential of thermoelectric technology for waste heat recovery from an economic point of view, the production costs have to be estimated and compared with the calculated target price per kW installed power of around 3'000 CHF/kW (compare section 6.3). In other words, the investment in the development and manufacturing of thermoelectric units for waste heat recovery applications makes only sense for the scenario of production costs being significantly below target price.

Thermoelectric units have a relatively low conversion efficiency (assumed to be 2.5% for the following calculations) which strongly limits their application range. In particular, thermoelectric units have only a significant potential in the low temperature range (as stated in section 4.6) due to more efficient competitive technologies in the high temperature range. The production costs are estimated for temperature difference of 40 °C, with a hot side temperature of 65 °C. The most suitable thermoelectric material for this condition is Bi_2Te_3.

The key components of the production cost are volume cost of the raw material and area manufacturing cost. Additionally costs such as assembly and heat exchangers are excluded from this first estimate.

Tellurium is expensive and currently costs about 117 $/kg[43], however the price is sub-

ject to strong annual fluctuations (peaking at 350 $/kg in 2011). The current price for bismuth is about 25 $/kg[45]. Taking into consideration the molar masses, Bi_2Te_3 costs about 70 $/kg.

For the calculation of the production cost, currency parity of USD, EUR and CHF is assumed. Based on a comparable research project in an EU country, the thermoelectric units are assumed to be produced as Bi_2Te_3 legs with a diameter of 4 mm and a height of 2 mm. [77]

The output power density of Bi_2Te_3 based thermoelectric generators for a temperature difference of 40 °C in an ideal scenario, assuming a thermoelectric conversion efficiency of 2.5% (see Fig. 1) and a heat transfer coefficient of the heat exchanger of 1'000W/m^2K, results in 1000W/m^2. To calculate a more realistic scenario however, information from commercially available Bi_2Te_3 modules from Thermonamics[78] were analysed and resulted in an output power density of 250 W/m^2. Based on this conservative scenario for the output density and taking into account the density of Bi_2Te_3 and assuming a fill factor of 1, the gravimetric power density of Bi_2Te_3 tablets is 16 W/kg for a height of 2 mm and 8 W/kg for a height of 4 mm. This leads to raw material costs per electrical output power unit of 4'300 CHF/kW of Bi_2Te_3 units with a height of 2 mm.

Industry experts provided rough estimates for the area manufacturing costs of Bi_2Te_3 legs (height 2mm). The manufacturing steps for thermoelectric units have two significant cost drivers: the melting and sintering process (reference - expert meeting with Jens Huber of Dr. Fritsch). These two processes constitute 1/3 each of the total manufacturing costs for Bi_2Te_3 legs, with the remaining steps such as mining, grinding etc. constituting the remaining 1/3. Detailed analysis for a comparable research project confirmed sintering cost of 0.008 EUR/leg. These costs include depreciation (otherwise reduced by factor of 2) and could be reduced to 0.004 EUR/table for large-scale production (40 million Bi_2Te_3 legs per year). Using a conservative approach and assuming manufacturing costs of 0.024 EUR/ leg results in an area production cost of 1'500 EUR/m^2. These area production costs are significant, consid-

ering that research is under way to reduce the area production cost for photovoltaic (PV) cells to around 50 to 140 $/m^2 [79]. With the conservative scenario output power density of 250 W/m^2 the manufacturing costs per unit of electrical output power are 6'000 CHF/kW for thermoelectric generators based on Bi_2Te_3 legs with a height of 2mm.

The production costs including the raw material costs are around 10'300 CHF/kW and therefore more than three times the amount of the target price per kW installed power. These production costs are indirectly confirmed by the sales prices of providers of commercial Bi_2Te_3 thermoelectric modules, charging for 1W modules around 14 $.[80] It can already be concluded that area manufacturing costs alone are currently significantly higher than the target price of 3'000 CHF/kW. It needs to be noted however that under the ideal scenario for the output power density, the production costs could potentially be reduced by a factor of 4 and would consequently become comparable to the target price. To further exploit the economic potential of Bi_2Te_3 based-thermoelectric units, the manufacturing costs would have to be significantly reduced (around a factor of 5), while the material costs for Bi_2Te_3 would need not to increase. If however the electricity price increases by a factor of 5 to around 0.50 CHF/kWh the exploitation of thermoelectric technology for waste heat recovery becomes economically viable at the current production costs.

6.5 Conclusion of economic feasibility

Although the market potential for waste heat recovery in the low temperature segment is huge, the economic feasibility for thermoelectric solutions is currently not given in the industrial waste heat recovery market: The estimation for production cost is roughly 3 times higher than the calculated target price. If costs for investments, marketing and distribution are added, the difference would be even higher.

As the sensitivity analysis has shown, there is no realistic on-grid scenario available, which would change the evaluation. The most likely one is a substantial increase of the elec-

tricity price: nevertheless also in this scenario the price for electricity would have to increase by a factor 5. Electricity prices higher than 0.50 CHF/kWh might however be found in off-grid-applications.

7. Potential applications for thermoelectric generators in building technology

In buildings air conditioning and cooling of machinery e.g. server stations, produce waste heat, which is investigated in this chapter on economic and feasibility aspect.

7.1. Economic aspects for applications within buildings versus industry and incineration plants

Machines in the industrial sector are constantly modified and upgraded due to the fast pace of technology development. The primary purpose of a production line in the industry is to manufacture products. Payback time for any investments into production lines have therefore to respect the product cycles. Nowadays the maximum accepted payback time in manufacturing is typically smaller than five years.

The primary purpose of waste incineration plants is the production of heat by the combustion of wastes. The live time of a waste incineration plant is calculated to be 20 to 40 years. Therefore payback times of investments into incineration plants are accepted to be about 10 years.

In contrast, the lifespan of buildings is much longer. House structures in Switzerland are defined to endure 100 years and installations of building technology roughly 40 years as by Swiss Standard SIA 480[81]. Thus investments into building technology allow a payback time of up to 25 years.

Table 11: Investment payback time in different sectors

Application	**Life time in years**	**Disposed payback time in years for investments**
Industrial production	10	5
Municipal incineration	20 to 40	10
Building technology	40	25

7.2. Economic calculations according to Swiss standard SIA 480

The Swiss standard 480:2004 released by SIA, Schweizerischer Ingenieur- und Architektenverein, gives a clear and reliable lifespan for different objects in and on buildings. For the installations of building technology a life time of 40 years is generally assumed.[82]

Based on table 11 and reference 83 (SIA 480:2004), thermoelectric generators within installations of building technology benefit from a longer payback time. Thus we focus on applications within building technology.

7.3. Most natural applications within buildings

7.3.1 Cold storage warehouses

Cold storage warehouses are well suited for the application of thermoelectric generators. In Neuendorf SO are three cold storage warehouses from the Swiss retailer Migros with a surface of 325'000 m^2 and an engine power of 2.7 MW_{el} for cooling incoming goods and keeping the inside temperature to -26°C[83]. It takes 3 MWh_{el} to lower the temperature of the cold storage warehouses by1 °C.[84,85]

The waste energy (hot air) of a cooling cycle is about three times of the energy of the electrical input for the cooling heat pump. Assuming that the heat to be removed from a room to be cooled amounts up to 2 kW, we need 1 kW electrical power for the heat pump resolving in 3 kW of waste heat to be transferred into the environment. Because of the in- and output of merchandise – cold goods leaving the storage and warm goods coming into the storage – a better thermal insulation will not result in a much lower cooling power. Therefore the electric energy produced by a thermoelectric generator is a perfect chance to increase the efficiency of the cooling system.

Assumption: With an average waste heat flow of 4 MW_{th} over the year, the accumulated waste heat would amount to 35GWh_{th} per year. The heat cooled down by an outside air

temperature of 9°C in average over the year[86] and assuming a temperature of 65°C at the hot side of the heat pump, the temperature difference seen by a thermoelectric generator would in average be around 56 °C. With an assumed efficiency of 2.5% for the thermoelectric generator, 875 MWh_{el} can be produced each year – which corresponds the electrical consumption of 160 households in Switzerland – and could be used for the operation of the cold storage warehouses.

7.3.2 Cooling of computer server rooms

Server rooms have strict regulations for the cooling of its components due to risk management and complex design requirements. Conventional server rooms are cooled with air cycles which transport the heat via a heat pump as waste heat to the environment. In the very cases that ground water is applied as a cooling medium, it's easy to introduce a thermoelectric generator into the plate heat exchanger.

7.3.3 Air conditioning in summer

Air conditioners within buildings are only used in summer when the temperatures are high. Assuming a waste heat flow at a temperature of 65°C on the hot side of the air conditioner and a temperature of 25°C of the environment in which the waste heat is released into, it would lead to a temperature difference of only 40 °C. This difference is still suitable for thermoelectric generators. Possible applications of thermoelectric generators with air conditioners might be in large buildings with customized air conditioners and ground water as cooling medium and should be investigated in a separate study.

8. Further potential applications for thermoelectric generators

Further possible applications for thermoelectric generators are within large inverters of power plants. Also in the automobile sector integrated into the exhaust gas line, thermoelectric generators could be used to convert waste heat into valuable electricity. These areas could be investigated in a separate study, as we focus in the following section to offshore ships with large electrical and thermal power and thus a sector with a huge potential.

8.1. Thermoelectric generators in cooling of ship propulsion systems

Thermoelectric generators for offshore ships have a great potential, as waste heat generated by the propulsion system is cooled down by seawater. A thermoelectric generator could be applied in the heat exchanger of this cooling system. The electric energy produced by the thermoelectric generator can be used to feed the heating, ventilation and air-conditioning system of the ship. The air-conditioning system itself also produces waste heat and could be equipped with thermoelectric generators, too.

Offshore ships have different cooling circulations with different cooling mediums at different temperatures which are kept separate. Table 11 shows three cooling cycles with possible temperatures on the hot and cold side of an installed thermoelectric generator.

Table 13: Temperatures of different cooling cycles to be used with a thermoelectric generator

Cooling medium	High temperature (cooling cycle)	Cold temperature (sea water)	Temperature difference available for thermoelectric generator
Cooling water	80 °C	20 °C	60 °C
Oil cooler	150 °C	20 °C	130 °C
Exhaust gases	220 °C	20 °C	200 °C

A typical offshore container ship with a diesel engine of 57’000 kW has an annual operation time of about 6480 hours (74%) at an average engine load of 36’500 kW

(64%)[87]. The heat loss is therefore 91’250 kW_{th} during operation time and the annual thermal energy loss 591’300 MWh_{th} assuming an efficiency of 40% for a diesel engine. Waste heat recovery systems are able to recover about 10% of the waste heat in electrical energy[88], as long as there are high temperature differences and high pressures[89]. Waste heat recovery systems are already available on the market. Coupling a thermoelectric generator to an existing waste heat recovery system would produce out of the lost heat additional 2’300 kW_{el} during operation time, resulting in 14’780 MWh_{el} per year – which corresponds to the electrical consumption of 2’700 households in Switzerland – and could be used for the operation of the heating, ventilation and air-conditioning system.

9. Design of a thermoelectric generator pilot plant for waste heat-recuperation

Fig. 14 shows a typical application of a cooling cycle with a heat pump extended with a thermoelectric generator.

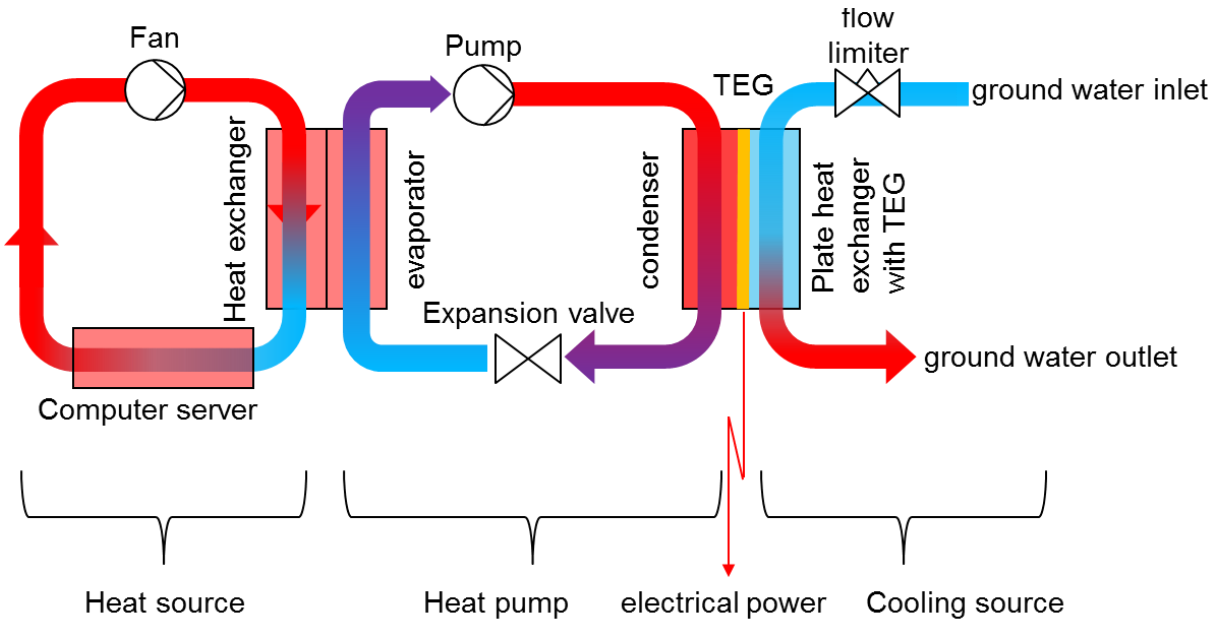

Figure 14: Simplified cooling cycle for a heat source, e.g. a server room, with thermoelectric generators.

The heat pump increases the efficiency of heat exchange between heat source and cooling source and lowers therefore the size and costs of the cooling cycle. The increased temperature difference between heat and cooling source allows the implementation of a thermoelectric generator in a plate heat exchanger for electric power production.

9.1. Goal of the pilot plant

To find an economically viable balance between heat conduction (and therefore size and costs of heat exchanger) and power generation (which lowers heat conduction), a pilot plant has been developed and built by W Neumann Consult AG. Different thermometers (2, 3, 4, and 5 in figure 10) together with the data sheet of the thermoelectric generator allow the calculation of the exact efficiency as a function the thermoelectric generator's properties.

The pilot plant is therefore a very practical tool to investigate and demonstrate the efficiency of newly designed thermoelectric generators in the temperature range below 65°C.

9.2. Design and properties of the pilot plant

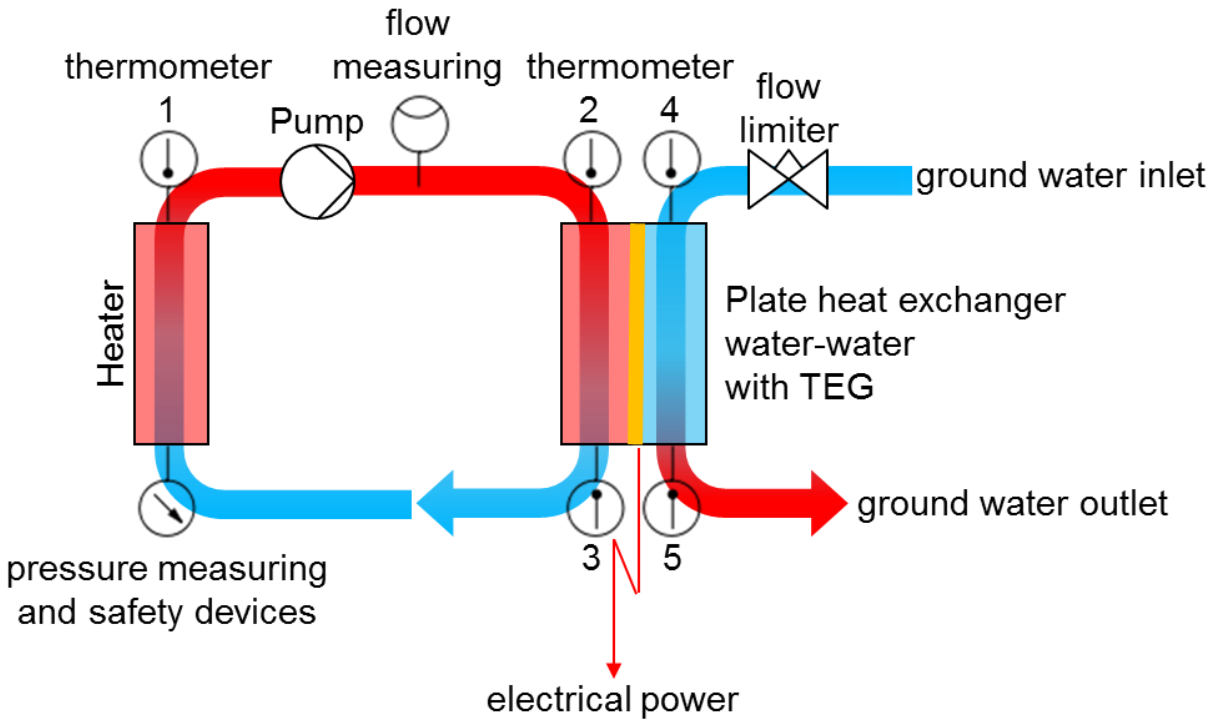

Figure 15: Schematic of the thermoelectric generator pilot plant simulating a typical cooling cycle

The pilot plant is designed for demonstration and research purposes. It has been developed with the following properties:

Table 14: Properties of pilot plant by W Neumann Consult AG

Component	Dimension	Value
Heater	W_{th}	1'000
Pump	W	3…70
Hot water flow	L/min	1…8 (dynamic)
Cold (ground) water flow	L/min	2 (static) ; 2…4 (dynamic)
Max area for TEG	cm^2	104
Max pressure hot water	bar	2.4
Max temperature hot water (thermometer 1)	°C	~ 95
Temperature hot water inlet (Thermometer 2)	°C	~ 55
Temperature hot water outlet (Thermometer 3)	°C	~ 50
Temperature cold water inlet (Thermometer 4)	°C	~ 10
Temperature cold water outlet (Thermometer 5)	°C	~ 20
Efficiency	W_{el}/W_{th}	To be determined during tests

The pilot plant includes besides the adjustable parameters also safety devices such as flow limiters, overpressure protection, expandable tubes and thermal sensors within the heater. On the electrical part, safety is maximized with separate sockets for heater and pump and an emergency mushroom pushbutton. LED's are built in for demonstration purposes, while a power meter equipped with a memory card allows collecting and processing data on a separate computer.

10. Conclusions

While at first sight, the potential for industrial waste heat recovery by thermoelectrics appears enormous, the results of the present study show that the main opportunities for thermoelectrics are in the low temperature segment, in which competing technologies become inefficient. In an industrial environment, process heat at a temperature above 65°C is most efficiently used by transferring it to preheat another process or by converting it into electric power via water steam cycles or at lower temperatures via organic Rankine cycles operating very close to the Carnot efficiency. In the temperature range below 65°C exists a huge opportunity for thermoelectrics as the conversion efficiencies of cycle processes becomes low.

Finding an economically viable route to tap into the gigantic potential of low grade waste heat at hot side temperatures at or below 65°C remains challenging. Our analysis suggests an average target price per kW installed power in the industrial environment on the order of 3’000 CHF/kW assuming a payback time of less than 5 years. Nevertheless, assuming a realistic output power density of 250 W/m^2, production costs of currently available thermoelectric generators are estimated at 10'300 CHF/kW and are consequently too high to obtain a positive business case. In the case of Bi_2Te_3, which is currently the only thermoelectric material exhibiting reasonably high zT values at this low temperatures, the raw materials costs contribute about half to the overall production cost due to the high cost of tellurium.

One of the major obstacles to render thermoelectrics economically viable in the industrial environment is the relatively short payback time of typically 5 years or less. Municipal incineration plants offer better conditions with 10 years payback time. The financial calculations for applications in the building sector are expected to be even more advantageous with typical payback times of 25 years. The market potential for the application of thermoelectric generators in the building sector is substantial. The needs and dynamics of this market deserve a closer look through further investigations. Yet another application to be explored in more detail is the implementation of thermoelectrics into the propulsion system of offshore ships,

where cooling can be achieved by seawater.

Challenges exist also on the materials side. Waste heat in buildings, arising from climate control units, is typically released into the outside environment at temperatures near 65°C, making Bi_2Te_3 based thermoelectric materials the best choice. Scaling Bi_2Te_3 based thermoelectric technology to the global building environment is expected to result in a significant pressure on the cost of tellurium requiring the development of tellurium free materials. Hope that such an alternative material may exist is given by the recent developments in the MgAgSb material system. However, from a cost point of view, the use of silver in thermoelectrics is even more prohibitive than the use of tellurium.

Other applications for which thermoelectrics may become economically viable are in off-grid or on-board applications. Electricity prices per kWh need to be at least a factor of 5 higher than grid electricity prices (currently 0.10 CHF/kWh). Legal regulations on CO_2 emissions may become another important driver to favor the integration of thermoelectric generators in these applications. For these applications, waste heat may be generated at temperatures above the maximum temperature for Bi_2Te_3 based materials (e.g. in an exhaust gas system of a gasoline engine) rendering the development of alternative materials with higher thermal stability essential. Candidate materials include skutterudites, Half-Heuslers, and the combination of tetrahedrites with magnesium silicides. Maximum zT for lead telluride based thermoelectric materials is reached at temperatures midway between the zT maxima of Bi_2Te_3 and the higher temperature material classes. This renders lead telluride an interesting material from a technological point of view. However, the use of lead telluride in thermoelectric converters is prohibited in Europe. Further materials research is necessary to develop a thermoelectric material consisting of abundant non-toxic elements that performs well at relatively low temperatures while exhibiting a high thermal stability.

11. Appendix

11.1 Industries with waste heat of 250°C

To investigate the estimated potential of waste heat in the 250°C temperature range, interviews were conducted with company representatives and supplemented by research data.

Case study 1: chemical industry

The company uses its 250°C heat source to generate steam. Any surplus heat flows are transmitted onwards for district heating. The cold and heat sources are spread across the company's entire site (50 ha), with the unused heat usually being under 100°C. Concentrating the various flows would be too expensive and much too laborious and would be uneconomical even with 100 sites. Water from the Rhône is used as the cold source and has a return flow at a temperature of 15–20°C.

Conclusion: This company already uses waste heat in the 250°C temperature range.

Case study 2: food and personal care industry

As the company has no interim storage facilities and makes modifications to its products on an ongoing basis, it operates a batch process. To melt fat and oil, the mixer is heated to around 100°C; the mixture is then at about 75°C and is cooled to room temperature (around 25°C). Ice water and cooling towers are used for the cooling process. Manufacturing operations are connected to a district heating network.

Conclusion: This company does not have any 250°C heat sources.

Case study 3: steel industry

The cooling system runs at low temperatures (30–40°C) on both the inflow and return flow sides. The hot gas in the furnace, which reaches temperatures of several hundred degrees Celsius, would have to be separated out in order to get to 250°C. In other words, this would require additional investment, which is not an attractive option for the company. Several measures for using waste heat are already planned.

Conclusion: Waste heat in the 250°C temperature range is either already used in this company or cannot be separated out.

Case study 4: information technology industry

To optimize energy efficiency, the temperature inside one of the data centers is to be increased from 22 to 26°C, which would reduce the power used for heating, ventilation and air-conditioning by around 42 per cent[90] (cf. SwissEnergy/SFOE 2004).

Cooling is performed by chillers that use groundwater cooling and waste heat. If heating is required inside the building, waste heat from the chillers is used; if no heating is required, groundwater is used for cooling. Waste heat with a temperature of 52/42°C (inflow/return flow) is used to heat the rooms. [91]

Conclusion: The heat source is outside the desired 250°C range and is already used to heat the building. Data centers also fall outside the scope of the research into industrial waste heat but were included in the study due to the waste heat that they generate at low temperatures.

SFOE study: waste heat in Swiss companies

An SFOE study looked at waste heat in nine companies. All generate this heat mainly at low temperatures (30–40°C), which prevents it from being used without any further intervention. However, central or local heat pumps can be used to raise the waste heat to a higher, usable temperature.

Conclusion: Industrial heat is rarely available at 250°C.

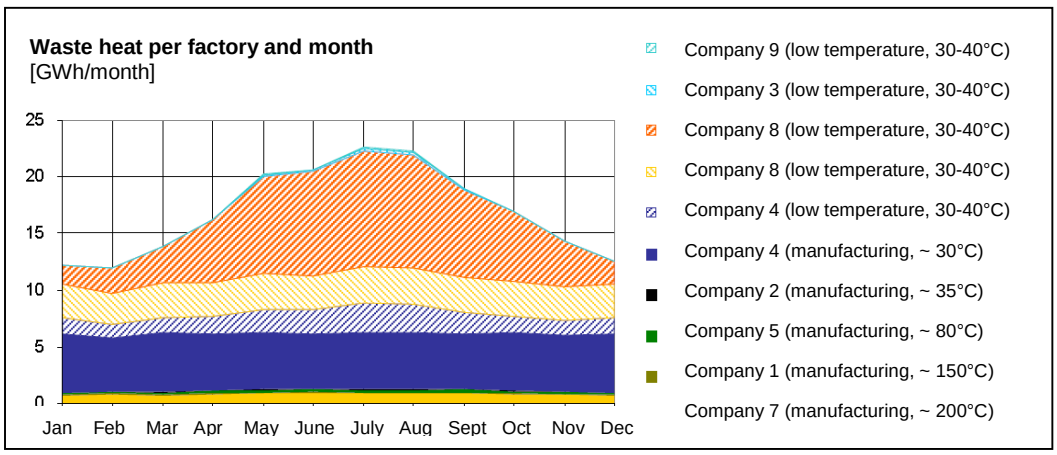

Fig. 9: Compilation of waste generated by nine Swiss companies.

[1] Art. 1.g. of the Swiss Energy Directive, https://www.admin.ch/opc/de/classified-compilation/19983391/index.html
[2] C. B. Vining, Nature 2009, 8, 83
[3] J. Yan, P. Gorai, B. Ortiz, S. Miller, S. A. Barnett, T. Mason, V. Stevanovic, and E. S. Toberer, Energy Environ. Sci. 2015, 8, 983
[4] H. Wang, Y. Pei, A. D. LaLonde, and G. J. Snyder, in Thermoelectric Nanomaterials, edited by K. Koumoto and T. Mori, p. 6, Springer, Berlin, 2013
[5] A. Bulusu, D. G. Walker, Superlattices and Microstructures 2008, 44, 1-36
[6] E. Altenkirch, Z. Phys. 1909, 10, 560
[7] A. F. Ioffe, Semiconductor Thermoelements and Thermoelectric Cooling, Infosearch, London
[8] H. S. Kim, W. Liu, G. Chen, C.-W. Chu, and Z. Ren, Proc. Nat. Acad. 2015, 112, 8205
[9] G. J. Snyder and T. S. Ursell, Phys. Rev. Lett. 2003, 91, 148301-1
[10] M. V. Vedernikov and E. K. Iordanishvili, Proc. 17th Int. Conf. Thermoelectrics, 1998, p.37-42, Nagoya, Japan
[11] B. Poudel, Q. Hao, Y. Ma, Y. Lan, A. Minnich, B. Yu, X. Yan, D. Wang, A. Muto, D. Vashaee, X. Chen, J. Liu, M. S. Dresselhaus, G. Chen, and Z. Ren, Science 2008, 320, 634
[12] S. I. Kim, K. H. Lee, H. A. Mun, H. S. Kim, S. W. Hwang, J. W. Roh, D. J. Yang, W. H. Shin, X. Sh. Li, Y. H. Lee, G. J. Snyder, and S. W. Kim, Science 2015, 348, 109
[13] R. Venkatasubramanian, E. Silvola, T. Colpitts, and B. O'Quinn, Nature 2001, 413, 597
[14] R. Venkatasubramanian, T. Colpitts, B. O'Quinn, S. Liu, N. El-Masry, and M. Lamvik, Appl. Phys. Lett. 1999, 75 1104
[15] Y. Z. Pei, J. Yang, L. D. Chen, W. Zhang, J. R. Salvador, and J. Yang, Appl. Phys. Lett. 2009, 95, 042101
[16] L. D. Chen, T. Kawahara, X. F. Tang, T. Goto, T. Hirai, J. S. Dyck, W. Chen, and C. Usher, J. Appl. Phys. 2001, 90 1864
[17] Y. Tang, Y. Qiu, L. Xi, X. Shi, W. Zhang, L. Chen, S.-M. Tseng, S.-W. Chen, and G. J. Snyder, Energy Environ. Sci. 2014, 7, 812-819
[18] Y. Tang, R. Hanus, S. W. Chen, G. J. Snyder, Nature Commun. 2015, 6, 7584
[19] H. Li, X. Tang, Q. Zhang, and C. Usher, Appl. Phys. Lett. 2009, 94, 102114
[20] Y. Shi, J. Yang, J. R. Salvador, M. Chi, J. Y. Cho, H. Wang, S. Bai, J. Yang, W. Zhang, and L. Chen, J. Am. Chem. Soc. 2011, 133, 7837-7846
[21] G. Rogl, A. Grytsiv, P. Rogl, N. Peranio, E. Bauer, M. Zehetbauer, O. Eibl, Acta Materialia 2014, 63 30-43
[22] G. Rogl, A. Grytsiv, P. Heinrich, E. Bauer, P. Kumar, N. Peranio, O. Eibl, J. Horky, M. Zehetbauer, and P. Rogl, Acta Materialia 2015, 91, 227-239
[23] Y. Tang, Z. M. Gibbs, L. A. Agapito, G. Li, H.-S. Kim, M. B. Nardelli, S. Curtarolo, and G. S. Snyder, Nature Materials in press, 2015
[24] T. Graf, C. Felser, and S. P. Parkin, Prog. Sol. State. Chem. 2011, 39, 1-50 and references therein
[25] S. Sakurada and N. Shutoh, Appl. Phys. Lett. 2005, 86, 082105
[26] C. Yu, T.-J. Zhu, R.-Z. Shi, Y. Zhang, X.-B. Zhao, J. He, Acta Materialia 2009, 57, 2757
[27] G. Joshi, X. Yan, H. Wang, W. Liu, G. Chen, and Z. Ren, Adv. Energy Mater. 2011, 1, 643-647
[28] J. P. A. Makongo, D. K. Misra, X. Y. Zhou, A. Pant, M. R. Shabetai, X. L. Su, C. Uher, K. L. Stokes, P. F. P. Poudeu, J. Am. Chem. Soc. 2011, 133, 10
[29] S. Populoh, M. H. Aguirre, O. C. Brunko, K. Galazka, Y. Lu, and A. Weidenkaff, Scripta Materialia 66, 2012, 1073-1076
[30] M. Schwall and B. Balke, Phys. Chem. Chem. Phys. 2013, 15, 1868

[31] C. Fu, T. Zhu, Y. Pei, H. Xie, H. Wang, G. J. Snyder, Y. Liu, Y. Liu, and X. Zhao, Adv. Energy Mater. 2014, 4, 1400600
[32] G. Joshi, R. He, M. Engber, G. Samsonidze, T. Pantha, E. Dahal, J. Yang, Y. Lan, B. Kozinsky, and Z. Reng, Energy Environ. Sci. 2014, 7, 4070-4076.
[33] C. Fu, T. Zhu, Y. Liu, H. Xie and X. Zhao, Energy Environ. Sci. 2015, 8, 216
[34] C. Fu, S. Bai, Y. Liu, Y. Tang, L. Chen, Y. Zhao, and T. Zhu, Nat. Comm. 2015, 6, 8144
[35] V. K. Zaitsev, M. I. Fedorov, E. A: Gurieva, I. S. Eremin, P. P. Konstantinov, A. Yu. Samunin, and Vedernikov, Phys. Rev. B 2006, 74, 045207
[36] W. Liu, X. Tan, K. Yin, H. Liu, X. Tang, J. Shi, Q. Zhang, and C. Uher, Phys. Rev. Lett. 2012, 108, 166601
[37] A. U. Khan, N. V. Vlachos, E. Hatzikraniotis, G. S. Polymeris, Ch. B. Lioutas, E. C. Stefanaki, K. M. Paraskevopoulos, I. Giapintzakis, Th. Kyratsi, Acta Materialia 2014, 77, 43.53
[38] X. Lu, D. T. Morelli, Y. Xia, F. Zhou, V. Ozolins, H. Chi, X. Zhou, and Ctirad Uher, Adv. Energy Mater. 2013, 3, 342-348
[39] E. J. Skoug and D. T. Morelli, Phys. Rev. Lett. 2011, 107, 235901
[40] X. Lu, D. T. Morelli, Y. Xia, and V. Ozolins, Chem. Mater. 2015, 27, 408-413
[41] H. Nowotny, W. Sibert, Z. Metallkd. 1941, 33, 391
[42] M. J. Kirkham, A. M. dos Santos, C. J. Rawn, E. Lara-Curzio, J. W. Sharp, and A. J. Thompson, Phys. Rev. B 2012, 85, 144120
[43] H. Zhao, J. Sui, Z. Tang, Y. Lan, Q. Jie, D. Kraemer, K. McEnaney, A. Guloy, G. Chen, Z. Ren, Nano Energy 2014, 7, 97
[44] H. Liu, X. Shi, F. Xu, L. Zhang, W. Zhang, L. Chen, Q. Li, C. Uher, T. Day, and G. J. Snyder, Nature Materials 2012, 11, 422
[45] US Geological Survey, http://minerals.usgs.gov/minerals/pubs/commodity/silver/mcs-2015-silve.pdf
[46] L.-D. Zhao, V. P. Dravid, and M. Kanatzidis, Energy Environ. Sci. 2014, 7, 251
[47] S. Populoh, O. Brunko, L. Karvonen, L. Sagarna, G. Saucke, P. Thiel, M. Trottmann, N. Vogel-Schäuble, and A. Weidenkaff, in Perovskites and related mixed oxides: concepts and applications, edited by P. Granger, V. I. Parvulescu, S. Calaiguine, W. Prellier, Wiley, 2016
[48] X. Mettan, R. Pisoni, P. Matus, A. Pisoni, J. Jacimovic, B. Nafradi, M. Spina, D. Pavuna, L. Forro, and E. Horvath, J. Phys. Chem. C 2015, 119, 11506-11510
[49] M. Culebras, C. M. Gomez, and A. Cantarero, Materials, 2014, 7, 6701-7632
[50] H. Keppner, S. Uhl, E. Laux, L. Jeandupeux, J. Tschanz, and T. Journot, Materials Today, Proceedings 2015, 2, 680
[51] US Geological Survey, http://minerals.usgs.gov/minerals/pubs/commodity/selenium/mcs-2015-tellu.pdf
[52] http://ec.europa.eu/growth/sectors/raw-materials/specific-interest/critical/index_en.htm
[53] US Geological Survey, http://minerals.usgs.gov/minerals/pubs/commodity/bismuth/mcs-2015-bismu.pdf
[54] US Geological Survey, http://minerals.usgs.gov/minerals/pubs/commodity/lead/mcs-2015-lead.pdf
[55] http://eur-lex.europa.eu/LexUriServ/LexUriServ.do?uri=CELEX:32002L0095:EN:HTML
[56] US Geological Survey, http://minerals.usgs.gov/minerals/pubs/commodity/cobalt/mcs-2015-cobal.pdf
[57] US Geological Survey, http://minerals.usgs.gov/minerals/pubs/commodity/antimony/mcs-2015-antim.pdf
[58] US Geological Survey, http://minerals.usgs.gov/minerals/pubs/commodity/rare_earths/mcs-2015-raree.pdf
[59] US Geological Survey, http://minerals.usgs.gov/minerals/pubs/commodity/zirconium/mcs-2015-zirco.pdf

[60] http://ec.europa.eu/growth/sectors/raw-materials/specific-interest/critical/index_en.htm
[61] US Geological Survey, http://minerals.usgs.gov/minerals/pubs/commodity/nickel/mcs-2015-nicke.pdf
[62] US Geological Survey, http://minerals.usgs.gov/minerals/pubs/commodity/niobium/mcs-2015-niobi.pdf
[63] www.alphabetenergy.com
[64] M. A. Green, K. Emery, Y. Hishikawa, W. Warta, and E. D. Dunlop, Prog. Photovolt.: Res. Appl. 2016, 24, 3-11
[65] http://www.nrel.gov/ncpv/images/efficiency_chart.jpg
[66] http://www.nature.com/authors/policies/solarchecklist.pdf
[67] H. Wang, W. D. Porter, H. Böttner, J. König, L. Chen, S. Bai, T. M. Tritt, A. Mayolet, J. Senawiratne, C. Smith, F. Harris, P. Gilbert, J. W. Sharp, J. Lo, H. Kleinke, L. Kiss, J. Electron. Mater.2013, 42, 654-664
[68] H. Wang, W. D. Porter, H. Böttner, J. König, L. Chen, S. Bai, T. M. Tritt, A. Mayolet, J. Senawiratne, C. Smith, F. Harris, P. Gilbert, J. W. Sharp, J. Lo, H. Kleinke, L. Kiss, J. Electron. Mater.2013, 42, 1073-1084
[69] K. A. Borup, J. de Boor, H. Wang, F. Drymiotis, F. Gascoin, X. Shi, L. Chen, M. I. Fedorov, E. Müller, B. B. Iversen, and G. Snyder, Energy & Environmental Science, 2015, 8, 423
[70] A. Heel et al., *Integration of a high temperature thermoelectric converter for electricity generation in a solid oxide fuel cell system (HITTEC)*, Swiss Federal Office of Energy, 2015
[71] T. Helbling and M. Bill, *Magneto-caloric machine for power generation – market opportunities and potential analysis*, Swiss Federal Office of Energy, 2014
[72] Authors, *Energiekaskade in der Industrie - Abwärmenutzung zwischen Industrieunternehmen*, Swiss Federal Office of Energy, 2011
[73] Wärmeverbund Rheinfelden Ost, https://www.aew.ch/content/dam/aew/downloads/waerme/AEW_Waermeversorgung_Waermeverbund_Rheinfelden_Ost.pdf.res/AEW_Waermeversorgung_Waermeverbund_Rheinfelden_Ost.pdf
[74] Victorinox, http://www.e-webtechnologies.com/sak/Victorinox_Media.pdf
[75] W. Neumann & Co, Potenzialanalyse zur Steigerung der Stromerzeugung, 2015
[76] P. Icha, Entwicklung der spezifischen Kohlendioxid-Emissionen des deutschen Strommix in den Jahren 1990 bis 2013, Umweltbundesamt, Dessau-Rosslau, 2014
[77] meeting Jens Huber from Dr Fritsch
[78] email exchange Mr Henry Zheng of Thermonamics
[79] J. Kalowekamo, E. Baker, Solar Energy 2009, 83, 1224
[80] product sheet Thermonamics http://www.thermonamic.com/pro.asp
[81] SIA, Wirtschaftlichkeitsrechnung für Investitionen im Hochbau, 2004, 26
[82] SIA 480:2004, Attachement B, Table 1, reference. 83
[83] https://www.espazium.ch/das-khlhaus-als-energiespeicher
[84] http://www.bfe.admin.ch/php/modules/publikationen/stream.php?extlang=de&name=de_999694365.pdf&endung=Wenn%20aus%20dem%20Tiefk%FChllager%20eine%20Batterie%20wird
[85] https://report.migros.ch/2014/integrierter-lagebericht/umwelt/energie-klima
[86] http://de.climate-data.org/location/155814
[87] MAN Diesel & Turbo, Waste Heat Recovery System (WHRS) for Reduction of Fuel Consumption, Emissions and EEDI, page 23, http://marine.man.eu/docs/librariesprovider6/technical-papers/waste-heat-recovery-system.pdf?sfvrsn=10

[88] MAN Diesel & Turbo, Waste Heat Recovery System (WHRS) for Reduction of Fuel Consumption, Emissions and EEDI, page 20, http://marine.man.eu/docs/librariesprovider6/technical-papers/waste-heat-recovery-system.pdf?sfvrsn=10
[89] MAN Diesel & Turbo, Waste Heat Recovery System (WHRS) for Reduction of Fuel Consumption, Emissions and EEDI, page 17-19, http://marine.man.eu/docs/librariesprovider6/technical-papers/waste-heat-recovery-system.pdf?sfvrsn=10
[90] A. Altenburger, *26°C in EDV-Räumen – eine Temperatur ohne Risiko, Merkblatt für Fachleute der HLK-Planung und EDV-Betreiber*, Swiss Federal Office of Energy, 2004
[91] City of Bern IT Services: Rechenzentrum der Stadtverwaltung Bern